

MARTIN MARIETTA ENERGY SYSTEMS LIBRARIES



3 4456 0366481 7

ORNL/TM-10767

ornl

**OAK RIDGE
NATIONAL
LABORATORY**

MARTIN MARIETTA

**Summary of ORNL Long-Term
Surveillance at the FFTF**

B. Damiano
J. A. Thie

OAK RIDGE NATIONAL LABORATORY
CENTRAL RESEARCH LIBRARY
CIRCULATION SECTION
4520N ROOM 175
LIBRARY LOAN COPY
DO NOT TRANSFER TO ANOTHER PERSON
If you wish someone else to see this
report, send its name with report and
the library will arrange a loan.
UCR 2065 (1-77)

MANAGED BY
MARTIN MARIETTA ENERGY SYSTEMS, INC.
FOR THE UNITED STATES
DEPARTMENT OF ENERGY

This report has been reproduced directly from the best available copy.

Available to DOE and DOE contractors from the Office of Scientific and Technical Information, P.O. Box 62, Oak Ridge, TN 37831; prices available from (615) 576-8401, FTS 626-8401.

Available to the public from the National Technical Information Service, U.S. Department of Commerce, 5285 Port Royal Rd., Springfield, VA 22161.

This report was prepared as an account of work sponsored by an agency of the United States Government. Neither the United States Government nor any agency thereof, nor any of their employees, makes any warranty, express or implied, or assumes any legal liability or responsibility for the accuracy, completeness, or usefulness of any information, apparatus, product, or process disclosed, or represents that its use would not infringe privately owned rights. Reference herein to any specific commercial product, process, or service by trade name, trademark, manufacturer, or otherwise, does not necessarily constitute or imply its endorsement, recommendation, or favoring by the United States Government or any agency thereof. The views and opinions of authors expressed herein do not necessarily state or reflect those of the United States Government or any agency thereof.

Instrumentation and Controls Division
SUMMARY OF ORNL LONG-TERM SURVEILLANCE AT THE FFTF

B. Damiano
J. A. Thie*

*Independent Consultant, Knoxville, Tennessee

Date published—August 1992

Prepared by
OAK RIDGE NATIONAL LABORATORY
Oak Ridge, Tennessee 37831-6285
managed by
MARTIN MARIETTA ENERGY SYSTEMS, INC.
for the
U.S. DEPARTMENT OF ENERGY
under contract DE-AC05-84OR21400



3 4456 0366481 7

CONTENTS

LIST OF FIGURES	v
LIST OF TABLES	vii
ABSTRACT	ix
1. INTRODUCTION	1
2. DATA COLLECTION SYSTEM	6
3. FFTF NOISE DATA STORED AT ORNL	12
4. DATA BASE IMPLEMENTATION	17
5. INTERPRETATION OF DATA	25
5.1 SIGNAL BACKGROUND	25
5.2 CONTROL ROD NOISE	29
5.3 FLOW RESONANCE AT 0.06 Hz	33
5.4 TEMPERATURE REACTIVITY NOISE	33
5.5 REACTIVITY RESONANCE AT 6.6 Hz	33
5.6 INTERFERING RESONANCES	37
5.7 PUMP PHENOMENA	41
5.8 OTHER RESONANCES	41
6. FUTURE POSSIBILITIES	43
7. ACKNOWLEDGMENTS	45
8. REFERENCES	46
Appendix A. EXAMPLES USING THE FFTF NOISE DATA BASE	49

LIST OF FIGURES

1.1	Locations of instrumentation used, with one of the three coolant loops shown	3
1.2	Cutaway view of the FFTF	4
2.1	Block diagram of ANSDS	7
2.2	ANSDS surveillance system hardware	8
2.3	Signal wiring diagram	9
4.1	Frequency intervals used to calculate rms ² values	19
4.2	FFTF data base tables and index columns used to relate data in different tables	24
5.1	Display at the loop 1 cold leg temperature channel in December 1985 at full power, showing how an asymmetrical 10-Hz signal from plant data acquisition equipment is superimposed on a random temperature fluctuation signal	26
5.2	Loop 1 and loop 2 pressures at full power and full flow, showing line frequency artifacts (including aliases) as well as real phenomena from the pumps' 16-Hz rotational frequency and 6 times this as the blade-passing frequency	27
5.3	The RMS neutron noise due to control rod fluctuation plotted against the relative worth of the inserted bank during the first fuel cycle	30
5.4	Spectra of LLFM-1 at full power and flow during fuel cycle 5	31
5.5	Spectra of neutron detectors at full power and flow during cycle 8	32
5.6	Low-frequency spectra of flow and neutron detectors at full power and full flow, showing their coherence at the flow's 0.06-Hz resonance	34
5.7	Low-frequency spectra of loop 1 flow and pressure at full power and full flow, showing their coherence at the 0.06-Hz resonance	35

LIST OF FIGURES (continued)

5.8	Coherence between an in-vessel fission chamber LLFM-2 and a vessel accelerometer at full power and flow in August 1983	36
5.9	Spectra taken in June 1984, showing how two LLFMs detect slightly different resonant frequencies (~11 Hz)	38
5.10	LLFM-1 and LLFM-2 in August 1983 exhibiting in-phase interference of two closely spaced resonances near 10 Hz	39
5.11	LLFM-1 and LLFM-3 in August 1983 exhibiting out-of-phase interference of two closely spaced resonances near 10 Hz	40

LIST OF TABLES

1.1	FFTF fuel cycles and control rods influencing noise	2
1.2	Characteristics of sensors used in analyses	5
2.1	ANSDS patch panel signals	10
3.1	Analog tapes of FFTF noise signals	13
3.2	ANSDS data files stored at ORNL	15
4.1	PSD frequency intervals	20
4.2	Tables and columns in FFTF noise data base	21

ABSTRACT

Oak Ridge National Laboratory has used an automated system between 1983 and 1987 to collect and analyze primary system noise data at the Fast Flux Test Facility (FFTF) located in Hanford, Washington. System operation and data handling are described, data collection efforts are summarized, and principal findings are presented. The following principal findings were obtained from the collected data.

1. The signals contain considerable contamination, especially the nonneutron detector signals. This contamination has complicated the task of data interpretation.
2. Primary pump effects are clearly observed in the pressure and neutron detector signals. Both rotational frequency and blade-passing frequencies can be clearly identified.
3. The development and verification of a model describing the contribution of control rods to low-frequency neutron noise is described.
4. A resonance at 0.06 Hz in the flow sensor signals is attributed to flow oscillations.
5. A resonance at 6.6 Hz in the neutron detector signals is attributed to lateral control rod vibrations.
6. A mathematical model describing the interference of closely spaced resonances excited by a common source is described. Model results are shown to closely match a phenomenon occurring near 10 Hz in the neutron detector signals.

Suggestions made regarding the direction of future work include

1. replacing the existing automated data collection system hardware and software to enable more versatile data collection activities to be performed;
2. expanding use of the existing FFTF noise data base, coupled with the collection and analysis of new data, to obtain insights into the noise phenomena; and
3. applying modeling techniques to develop an understanding of the physical nature of noise sources.

A list of potential applications of FFTF noise analysis, based on the successful applications of noise analysis in pressurized water reactors, is given and includes predicting control rod noise, detecting instrumentation degradation and failure, reducing the frequency of instrumentation surveillance tests, supplementing primary pump and reactor internals vibration monitoring by the use of process instrumentation, and monitoring for changes in the temperature coefficient of reactivity.

1. INTRODUCTION

An automated data collection system was used by Oak Ridge National Laboratory (ORNL) at the Fast Flux Test Facility (FFTF) at Hanford, Washington, between 1983 and 1987.¹ From the facility, a 400-MW(t) sodium-cooled fast test reactor,² noise in various primary system variables is spectral-analyzed on the data collection system. This report summarizes the operation of this system and presents some principal findings obtained from the data collected. An assessment of ongoing data handling and interpretation efforts as well as comments about further work are included.

Table 1.1 shows the fuel cycle history of the FFTF through 1987. The data collection system, described in the next section, began operating during the third fuel cycle. Prior to this cycle, neutron noise data were taken by plant personnel during initial startup and proved to be useful.³ In particular, noise analysis has proven helpful in determining excessive control rod vibration. Concurrent with ORNL's participation were continuing activities by site personnel in taking and interpreting neutron noise as influenced by control rods.^{4,5}

An overview of the FFTF showing the locations of transducers used in this work is shown in Figs. 1.1 and 1.2. The specific sensors and their characteristics are listed in Table 1.2, and more complete descriptions are in the literature.² While the neutron detectors were always among signals being analyzed, other transducer types were also used part of the time—more so in recent fuel cycles than in earlier ones.

The following sections describe how the data are collected, stored, and interpreted. Unique features of the data collection system and of the data themselves are the ability to control the data collection system remotely by commands transmitted by a modem over a telephone line and the use of a data base to manage the large volume of automatically collected data. An assessment of the understanding of the data and the usefulness of the tools it provides is presented in the final sections.

Table 1.1. FFTF fuel cycles and control rods influencing noise

Date	Fuel cycle	Control rods used
1982	1	Only normal FFTF rods present
1983 (first)	2	ADVAB-2
1983 (last)	3	ADVAB-2
1984 (first)	4	ADVAB-2 and ADVAB-1A
1984 (last)	5	ADVAB-2, ADVAB-1A, and ADVAB-1B
1985 (first)	6	ADVAB-1A and ADVAB-1B
1985 (last)	7	ADVAB-2, ADVAB-1A, and ADVAB-1B
1986	8	
1987 (first)	9	ADVAB-1A and ADVAB-1B, with the former as rod #9 before 3/87 but elsewhere after 3/87
1987 (last)	10	

Note: Special advanced absorber control rods (ADVABs) were used in place of one or more of the six normal FFTF rods. These ADVABs were found to influence low-frequency neutron noise significantly.

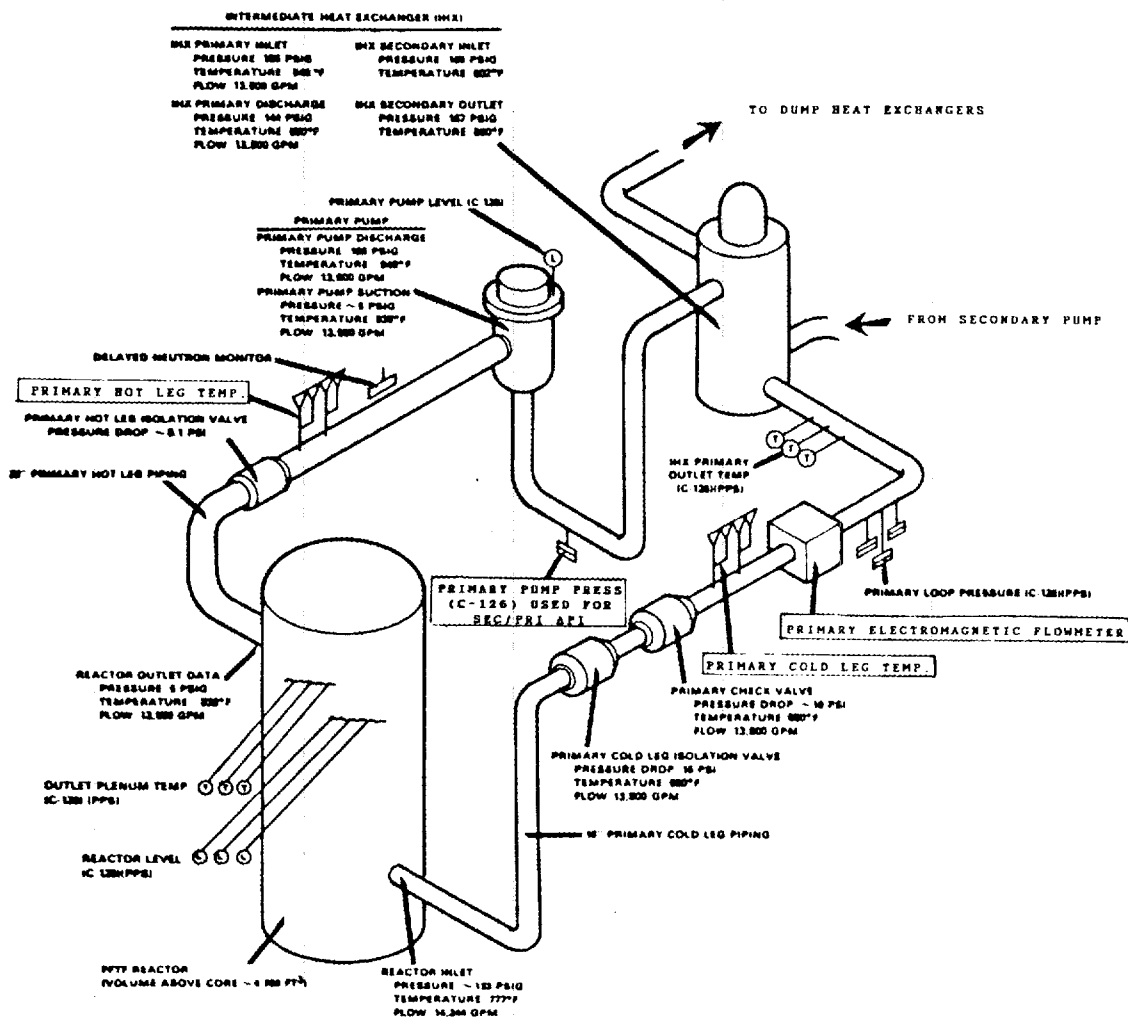


Fig. 1.1. Locations of instrumentation used, with one of the three coolant loops shown. Encircled are transducers used for noise analysis.

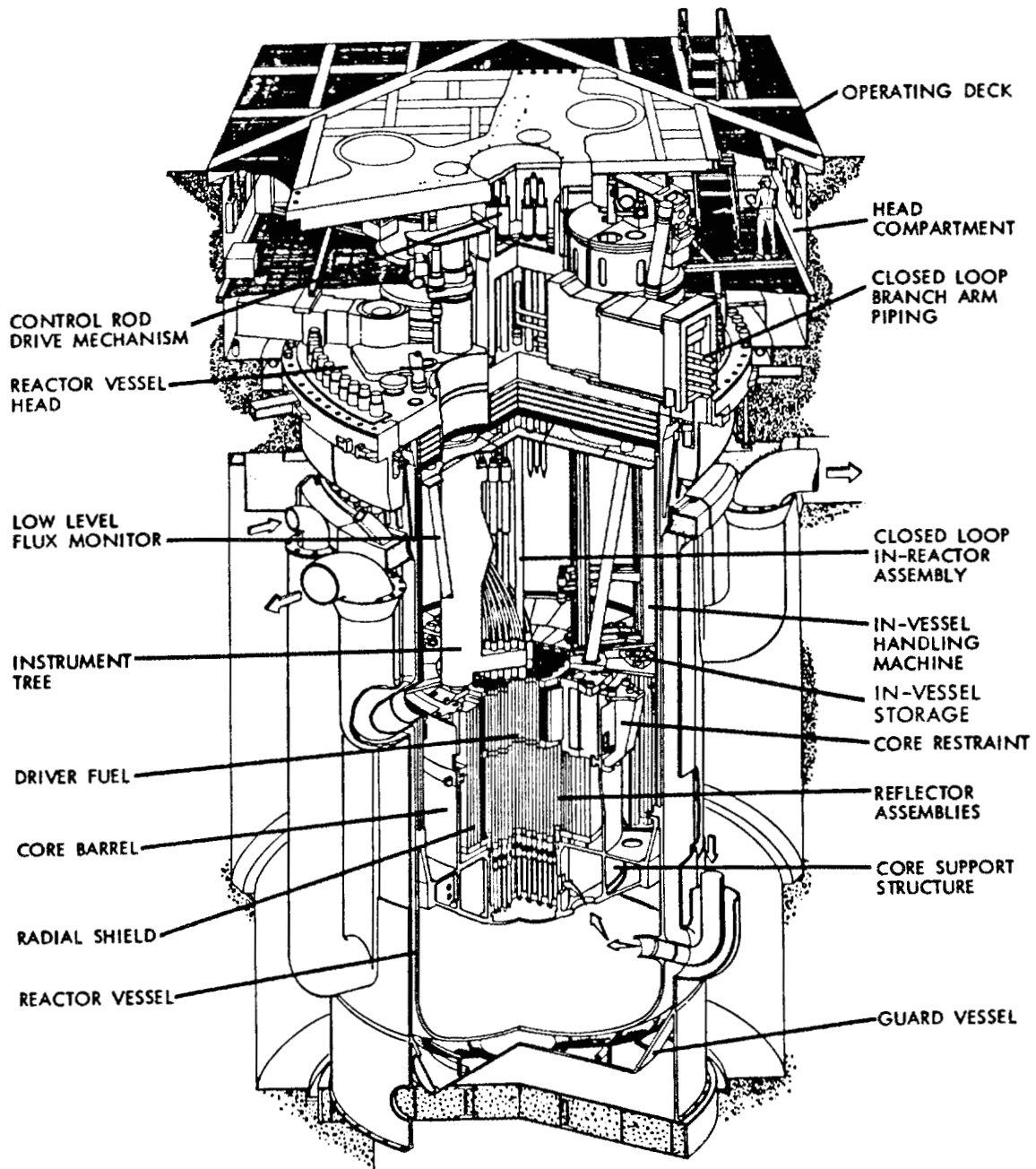


Fig. 1.2. Cutaway view of the FFTF, with representative locations of neutron and accelerometer transducers encircled.

Table 1.2. Characteristics of sensors used in analyses

Sensor (type) ^a	Location ^b	Calibration factor
LLFM-1 (fission counter)	In-vessel, loop 3 side	0.020 V/% power ^c
LLFM-2 (fission counter)	In-vessel, loop 1 side	0.020 V/% power ^c
LLFM-3 (fission counter)	In-vessel, loop 2 side	0.020 V/% power ^c
CIC-1 (ion chamber)	Ex-vessel, loop 3 side	0.079 V/% power
CIC-2 (ion chamber)	Ex-vessel, loop 1 side	0.079 V/% power
CIC-3 (ion chamber)	Ex-vessel, loop 2 side	0.079 V/% power
Cold leg 1,2,3 (RTD)	Loop 1,2,3	0.001 V/°F
Hot leg 1,2,3 (RTD)	Loop 1,2,3	0.001 V/°F
Flow 1,2,3 (electromagnetic flowmeter)	Loop 1,2,3	0.238 V/K-gpm
Pressure 1,2 (strain gage and diaphragm)	Loop 1,2	0.016 V/psi
Accelerometer at control rod mechanism top or bottom	Above vessel	
Accelerometer on the vessel	On vessel	

^aLLFM is a low-level flux monitor; CIC is a compensated ion chamber; RTD is a resistance temperature detector.

^bSee also Figs. 1.1 and 1.2.

^cFactors for the usual at-power withdrawn instrument position in its thimble.

2. DATA COLLECTION SYSTEM

The automated noise surveillance and diagnostic system (ANSDS) consists of several major components. A PDP-11/34A minicomputer with 96 K-words of random access memory is used to perform analysis and to control operation of other system components. Program and data file storage is provided by two RK05-type disk drives (one RK05F disk drive with two fixed surfaces and one RK05J drive with one removable surface) with a total storage capacity of 7.5 Mbytes. The signal-conditioning portion of the system consists of 16 computer-controlled amplifiers including sample-and-hold circuitry), designed and built by the ORNL Instrumentation and Controls Division, and 16 Rockland Model 816 analog low-pass antialiasing filters. One Digital Equipment Corporation (DEC) DR11-K parallel input/output device is used to control the amplifiers and a second DR11-K controls the Rockland filters. Analog-to-digital conversion (ADC) is performed by an ADAC Model 600/AD ADC converter in conjunction with a DEC KW11-P programmable clock and amplifier sample-and-hold circuitry. The maximum ADC rate is 100,000 samples/s. The system can be controlled on-site using a Tektronix 4006 terminal or remotely using a modem and telephone line. A block diagram of the ANSDS hardware is shown in Fig. 2.1. Figure 2.2 is a photograph of the ANSDS. A more detailed ANSDS hardware description is given in ref. 6.

Figure 2.3 is a wiring diagram of the reactor noise signals between the FFTF control room and the ANSDS. Originating at a control room patch panel, the monitored signals pass through isolation amplifiers before being routed to an intermediate patch panel. The neutron signals, in addition to passing through the isolation amplifiers, also are conditioned with a 20-Hz low-pass filter to avoid aliasing. The signals are then routed to the data acquisition room (room 404) where they are available for a Hanford Engineering Development Laboratory (HEDL) surveillance system and to the ANSDS patch panel. Thus, as can be seen from Fig. 2.3, the possibility exists for the ANSDS signals to be contaminated with interference from either HEDL or control room surveillance equipment. The 24 signals available at the ANSDS patch panel are listed in Table 2.1.

The ANSDS initially performed continuous on-line monitoring of FFTF noise signals using the Power Spectral Density Recognition (PSDREC) Continuous Reactor Surveillance Program developed at ORNL. PSDREC employs a statistically based pattern recognition system for surveillance of reactor signals.⁶ This system uses auto-power spectral density values (PSDs) to characterize the condition of the monitored equipment. A statistically based comparison between current PSDs and baseline (normal) PSDs is used to detect off-normal conditions. If a suspect condition is detected, the suspect PSDs and information indicating the reactor conditions are stored on disk for later examination by a noise analyst. Previous to its application at the FFTF, PSDREC was used to perform long-term surveillance at the Sequoyah-1 nuclear power plant.⁷ During this period (between the installation of the ANSDS in 1983 and December 1985), several analog tape recordings of FFTF noise data were made by ORNL personnel so that cross-spectral analysis could be performed at selected times.

After December 1985, the ANSDS was operated as a remotely controlled noise data acquisition system operated from ORNL. An advantage of this latter mode of operation was the addition of cross-power spectral density calculation. The ANSDS can simultaneously collect and store noise data for up to four signals. Data are stored in the

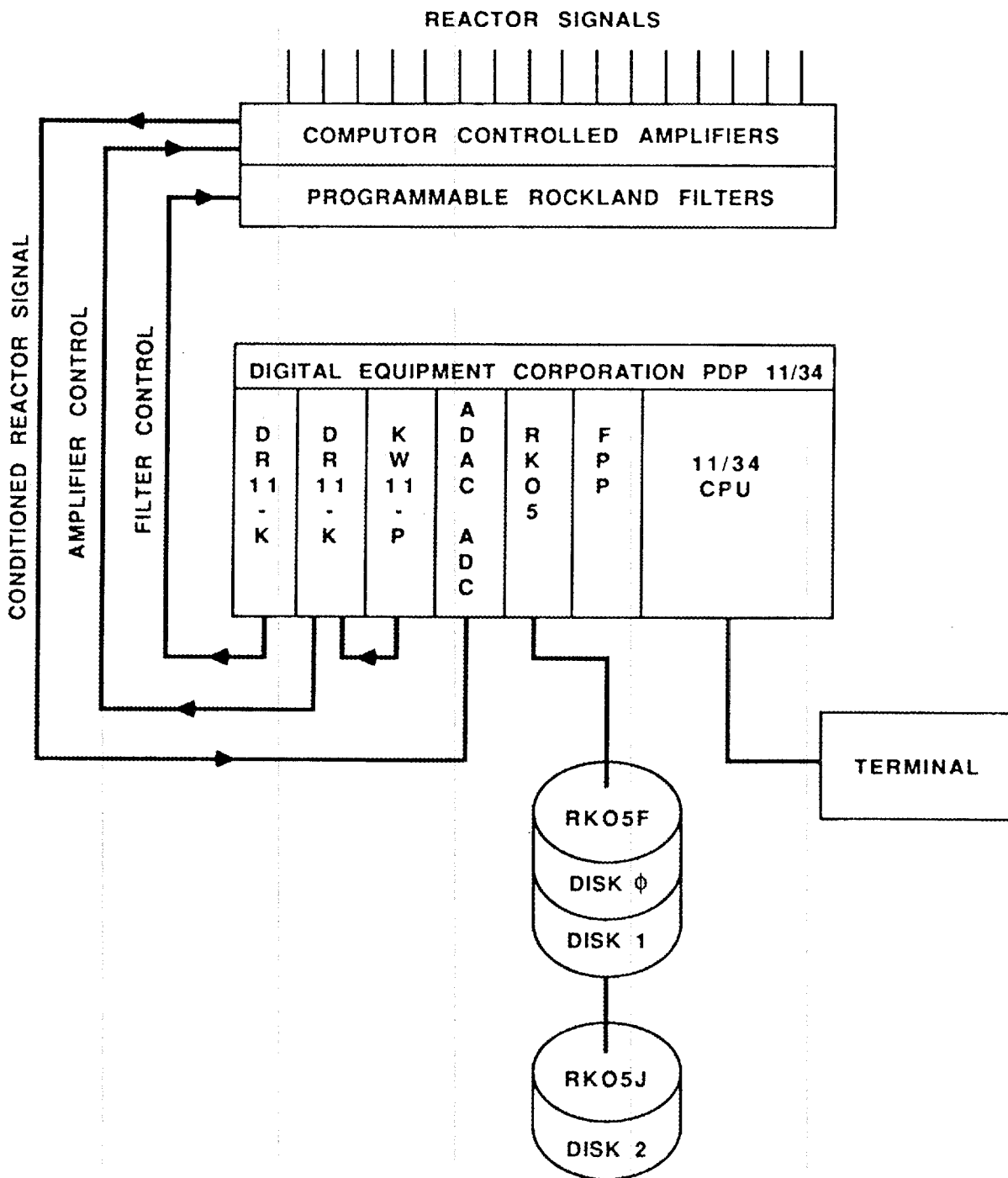


Fig. 2.1. Block diagram of ANSDS.



Fig. 2.2. ANSDS surveillance system hardware.

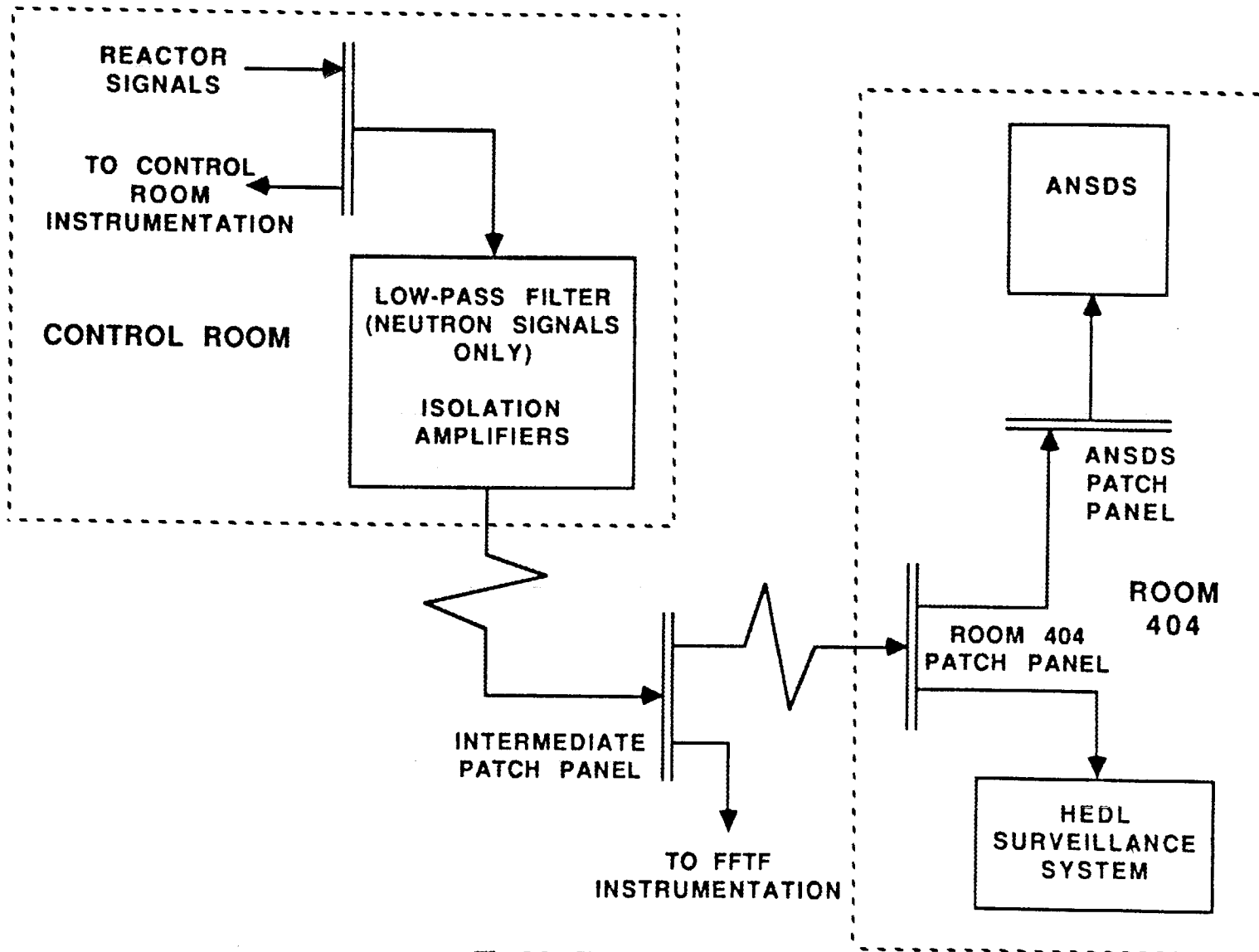


Fig. 23. Signal wiring diagram.

Table 2.1. ANSDS patch panel signals

Patch panel position	Signal name	Engineering units ^a
1	Loop-1 primary flow	K-gpm ^b
2	Loop-2 primary flow	K-gpm
3	Loop-3 primary flow	K-gpm
4	Loop-1 secondary flow	K-gpm
5	Loop-2 secondary flow	K-gpm
6	Loop-3 secondary flow	K-gpm
7	Loop-1 primary hot leg temperature	°F
8	Loop-1 primary cold leg temperature	°F
9	Loop-2 primary hot leg temperature	°F
10	Loop-2 primary cold leg temperature	°F
11	Loop-3 primary hot leg temperature	°F
12	Loop-3 primary cold leg temperature	°F
13	Loop-1 IHX ^c inlet pressure	psi
14	Loop-2 IHX inlet pressure	psi
15	Loop-3 IHX inlet pressure	psi
16	LLFM-1 count rate	volt
17	LLFM-2 count rate	volt
18	LLFM-3 count rate	volt
19	LLFM-1 (loop-3)	volt
20	LLFM-2 (loop-1)	volt
21	LLFM-3 (loop-2)	volt
22	CIC-1 (loop-3)	% full power
23	CIC-2 (loop-1)	% full power
24	CIC-3 (loop-2)	% full power

^aUnits as stored in the Au, FFTF noise data base.

^bK-gpm = 1000 gal/min.

^cIHX = intermediate heat exchanger.

form of PSDs and cross-power spectral densities (CPSDs). In addition to the PSDs and CPSDs, each signal's amplifier gain and antialiasing filter cutoff frequency are stored, as well as the clock time, the reactor state determined from the reactor signals measured at the beginning and end of each data collection period, and the sampling rate, block size, and number of blocks.

ANSDS output data files consist of multiple data sets. Parameters used to control collection for each data set, as well as the number of data sets in a data file, are contained in a control parameter file. These parameters control either sampling for the entire data set or individual data channel signal conditioning. Parameters controlling data set collection are the number of blocks, block size, sampling rate, and number of channels. Parameters controlling data channel signal conditionings are the channel number (which specifies the reactor signal connected to each amplifier), amplifier coupling mode, amplifier gain, and cutoff frequency of the antialiasing filter. These parameters for multiple data sets may be "stacked" in the control parameter data file, allowing consecutive data collections to be performed. Output data files were stored on a removable RK05J disk. These disks were periodically shipped to ORNL for analysis and storage.

3. FFTF NOISE DATA STORED AT ORNL

Analog tape recordings of FFTF noise signals were made during 1983 and 1984, and the resulting tapes, stored at ORNL, are summarized in Table 3.1. Each tape had calibration signals recorded before any noise data were taken. Documentation of the equipment, time, reactor state, and location on the tape of data and calibration signals were recorded on each tape.

Data collected by the ANSDS during 1986 and 1987 are stored on seven RK05 disks that hold 59 data files containing approximately 8000 spectra. These data were collected under a variety of reactor power and flow conditions using various sensor combinations. The ANSDS has collected data during normal operation, tests, and between-cycle shutdowns. Normal operating data, generally collected weekly with the FFTF at full power and flow conditions, are intended to provide a record of the normal fluctuations in the FFTF noise signals. Noise data collected during tests at the FFTF are intended for analysis of test effects on reactor noise in the hope that they will lead to a better understanding of FFTF noise sources. During tests, the ANSDS collected data continuously using many sensor combinations. As a result, the large volume of data collected over a short time allows a detailed examination of test effects on reactor noise signals.

Tests have generally involved off-normal power/flow combinations or unusual control rod configurations. A series of tests performed in February and March of 1986 allowed noise data to be collected for reactor powers ranging between 0 and 100% of full power and primary flows ranging between 65 and 100% of full flow.

The ANSDS collected noise data during two control rod tests in 1987. Using different core positions, an advanced absorber control rod (ADVAB-1A or ADVAB-1B) or a standard FFTF control rod was inserted and then withdrawn in 2-in. increments while remaining control rods were maneuvered to keep the reactor power at 90%.

Data were collected during the between-cycle shutdown occurring in October and November of 1987. These data should be useful for determining whether any given effect seen in the FFTF signals is real or is some form of background artifact. A summary of data type, reactor conditions, and date for each ANSDS output data file collected since December 1985 is shown in Table 3.2.

Table 3.1. Analog tapes of FFTF noise signals

Tape No.	Date	Signal	Amp gain	Filter	Conditions		
10	4/18/83	LLFM-1	100	20	91% power, 100% flow		
		LLFM-2	100	20			
		CIC-1	20	20	3.75 ips ^a tape speed		
		CIC-2	20	20			
374	8/10/83	LLFM-1		32	20100% power, 100% flow		
		LLFM-2	32	20			
		LLFM-3	32	20	Data includes control rod movements		
		CIC-1	8	20			
		CIC-2	8	20	15/16 ips ^a tape speed		
		CIC-3	8	20			
		ADVAB	1	20			
		vert. accel-erometer					
	Vessel						
	vert. accel-erometer	1	20				
373	8/11/83	LLFM-1	32	20	100% power, 100% flow		
		LLFM-2	32	20			
		LLFM-3	32	20	Data includes control rod movements		
		CIC-1	8	20			
		CIC-2	8	20	3.75 ips ^a tape speed		
		CIC-3	8	20			
		ADVAB	1	2000			
		vert. accel-erometer					
			Vessel	1	2000		
			vert. accel-erometer				
	Time code ^b	-	-				

Table 3.1. (continued)

Tape No.	Date	Signal	Amp gain	Filter	Conditions
375	3/14/84	LLFM-1	64	30	100% power, 100% flow
		LLFM-2	64	30	Tape includes test of
		LLFM-3	64	30	ANSDS signal condi-
		CIC-1	16	30	tioning equipment
		CIC-2	16	30	using white noise
		CIC-3	16	30	
		Time code ^b	-	-	3.75 ips ^a tape speed

^aips = in./s.

^bTime code: time information was recorded directly on tape.

Table 3.2. ANSDS data files stored at ORNL

Data disk	File name	Date	Channel number ^a	Analysis number ^b	Conditions ^c
FFTF					
Data 1	DEC19.DAT	12/19/85	2	12	100% power, 100% flow
	FEB07.DAT	2/07/86	5(3), 12(2)	17	65% power, 95% flow
	FEB10.DAT	2/10/86	7(3), 15(2)	22	90% power, 95% flow
	FEB12.DAT	2/12/86	5(3), 3(2)	8	90% power, 95% flow
	FEB13.DAT	2/13/86	3(3), 6(2)	9	100% power, 100% flow
	FEB14.DAT	2/14/86	12(4), 2(2)	14	100% power, 100% flow
	FEB15.DAT	2/15/86	12(4), 2(2)	14	100% power, 100% flow
	FEB16.DAT	2/16/86	12(4), 2(2)	14	100% power, 100% flow
	FEB17.DAT	2/17/86	4	84	100% power, 100% flow
	FEB18.DAT	2/18/86	4	84	65% power, 65% flow
	FEB19.DAT	2/19/86	4	84	65% power, 95% flow
FFTF					
Data 2	FEB20.DAT	2/20/86	4	84	64% power, 78% flow
	FEB21.DAT	2/21/86	4	84	64% power, 95% flow
	FEB22.DAT	2/22/86	4	84	64% power, 67% flow
	FEB23.DAT	2/23/86	4	84	60% power, 100% flow
FFTF					
Data 3	FEB28.DAT	2/28/86	4	84	42% power, 66% flow
	MAR01.DAT	3/01/86	4	84	37% power, 95% flow
	MAR02.DAT	3/02/86	4	84	25% power, 65% flow
	MAR03.DAT	3/03/86	4	84	19% power, 95% flow
FFTF					
Data 4	MAR05.DAT	3/04/86	4	72	24% power, 65% flow
	MAR06.DAT	3/06/86	4	72	24% power, 95% flow
	MAR07.DAT	3/07/86	4	72	37% power, 95% flow
	MAR09.DAT	3/09/86	4	72	15% power, 73% flow
	MAR10.DAT	3/10/86	4	60	9% power, 96% flow
FFTF					
Data 5	DATA3.DAT	1/12/87	4	16	Control rod test
	DATA4.DAT	1/12/87	4	40	Control rod test
	DATA5.DAT	1/13/87	4	40	Control rod test
	DATA6.DAT	1/13/87	4	40	Control rod test
	DATA7.DAT	1/14/87	4	32	Control rod test
	DATA8.DAT	1/14/87	4	20	Control rod test

Table 3.2. (continued)

Data disk	File name	Date	Channel number ^a	Analysis number ^b	Conditions ^c
FFTF					
Data 6	MAR24.DAT	3/24/87	4	10	Normal operation
	APR6.DAT	4/06/87	4	10	Normal operation
	APR14.DAT	4/14/87	4	10	Normal operation
	APR20.DAT	4/20/87	4	10	Normal operation
	APR28.DAT	4/28/87	4	10	Normal operation
	MAY4.DAT	5/04/87	4	10	Normal operation
	MAY11.DAT	5/11/87	4	10	Normal operation
	JUN10.DAT	6/10/87	4	10	Normal operation
	JUN15.DAT	6/15/87	4	10	Normal operation
	JUL22.DAT	7/22/87	4	10	Normal operation
	SEPT10.DAT	9/10/87	4	10	Normal operation
	SEP151.DAT	9/15/87	4	32	Control rod test
	SEP152.DAT	9/15/87	4	32	Control rod test
	SEP162.DAT	9/16/87	4	32	Control rod test
	SEP163.DAT	9/16/87	4	32	Control rod test
	SEP171.DAT	9/17/87	4	32	Control rod test
FFTF					
Data 7	OCT7.DAT	10/07/87	4	32	Normal operation
	OCT13.DAT	10/13/87	4	32	Shutdown data
	OCT14.DAT	10/14/87	4	32	Shutdown data
	OCT15.DAT	10/15/87	4	32	Shutdown data
	OCT16.DAT	10/16/87	4	32	Shutdown data
	NOV10.DAT	11/10/87	4	32	Shutdown data
	DEC02.DAT	12/02/87	4	10	Normal operation
	DEC14.DAT	12/14/87	4	10	Normal operation
	DEC21.DAT	12/21/87	4	10	Normal operation
	JAN04.DAT	1/04/88	4	10	Normal operation

^aNumber of data signals for which power spectral densities (PSDs) are calculated. If all data sets in a data file do not calculate PSDs for the same number of signals, the expression A(B),C(D) appears. A(B),C(D) indicates that A data sets calculated PSDs for B signals and C data sets calculated PSDs for D signals.

^bNumber of data sets in the data file.

^cPower and flow values indicate interesting conditions at which data were collected. These conditions, in general, are not constant for all data sets in the data file.

4. DATA BASE IMPLEMENTATION

The FFTF noise data base uses the Oracle Data Base Management System,⁸ a commercially available data base software package operating on an IBM personal computer. A data base is used to organize, store, and recall the FFTF noise data because:

- The large volume of collected data makes visual examination and screening of data impractical;
- Selection of data meeting certain criteria is simple, fast, and thorough; and
- Data base implementation saves considerable space compared to storing volumes of hard-copy plots.

If hard-copy plots are needed to examine some feature of the noise data in detail, these can be generated using the original ANSDS output data files.

Increased data base efficiency is obtained by storing only features extracted from a PSD rather than the PSD itself; feature extraction, which is necessary for noise data comparison and interpretation, is not performed each time spectral data are recalled from the data base. Reference 9 was used as a guide in selecting the information stored in the data base.

The FFTF noise data base contains either documentation information or measurement values. The documentation information stored in the FFTF data base is

- time and date of data collection;
- identification of signals;
- data file of each data set;
- data set number;
- amplifier gains;
- frequency cutoffs of antialiasing filters; and
- sampling rate, block size, and number of blocks.

The measurement values stored in the FFTF data base are

- dc voltages indicating the reactor state, converted into engineering units, of each of the ANSDS noise signals, measured at both the beginning and the end of each data collection; and
- spectral information extracted from the PSDs.

A program was written to search PSDs for peaks and to compute the square of the root-mean-square (rms^2) values. Output from this program is used as data base input. Thus, these PSD peak frequencies and amplitudes, as well as the rms^2 within the frequency band selected, are the spectral features extracted for storage in the FFTF noise data base. The rms^2 values are calculated for 24 frequency intervals. The frequency interval number, in addition to identifying the rms^2 values, is also used to label and identify the PSD peaks that occur in the interval. For each frequency interval, space is reserved in the data base for one peak amplitude and frequency value for each PSD. Peak values are recalled by using the frequency interval number as identification. Experience has shown that more than one PSD peak will rarely occur in a frequency interval, but when this circumstance occurs, values corresponding to the higher frequency PSD peak are stored in the data base.

The 24 frequency intervals used to label the PSD peaks and calculate rms^2 values were selected after examining the location of PSD peaks in the low-level flux monitor, compensated ion chamber, intermediate heat exchanger (IHX) pressure transducer, and primary loop flow transducer signals during the full-power, full-flow operation of cycle 9. Peak frequencies below 20 Hz (the antialiasing cutoff frequency for these measurements) could be grouped into 11 frequency bands. Figure 4.1 shows the frequency range between 0.1 and 20 Hz divided into frequency intervals based on these frequency bands. The even-numbered intervals correspond to the 11 frequency bands containing the majority of the PSD peaks. The odd-numbered intervals are the parts of the 0.1- to 20-Hz frequency range remaining after the even-numbered intervals are formed. These 23 intervals, along with an interval from 0.1 to 20 Hz, are used to calculate rms^2 values and label peak features. Frequency intervals are listed in Table 4.1.

Data in the FFTF data base are divided into tables consisting of rows and columns. Columns contain table values for the same measurement quantity. Rows contain the column values collected during each data analysis period. Each table and its columns are listed in Table 4.2.

Upon inspection of Table 4.2, one finds that identical column names ending in "KEY" appear in more than one table. These columns, known as index columns, identify related information stored in more than one table. Values in the "MEASUREMENT_KEY" columns identify the data set from which rows in the table were extracted. Each data set is assigned a unique identification number when data set information is extracted from the ANSDS data files. Selecting rows with the same "MEASUREMENT_KEY" value recalls data extracted from the same data set.

Values in the "FILE_KEY" columns identify which ANSDS data file initially held the data base information. Each ANSDS data file is assigned a unique identification number. Selecting rows with the same "FILE_KEY" value recalls data extracted from the same data file.

Values in the "PATCH_KEY" columns identify the sensor used to make each measurement. Each sensor is assigned a unique number based on its signal's ANSDS patch panel position. Selecting rows with the same "PATCH_KEY" value recalls information measured by the same sensor.

Values in the "INTERVAL_KEY" columns identify the frequency interval used to identify each piece of spectral information in the data base. Selecting rows with the same "INTERVAL_KEY" value recalls information extracted from the same frequency interval.

INTERVALS

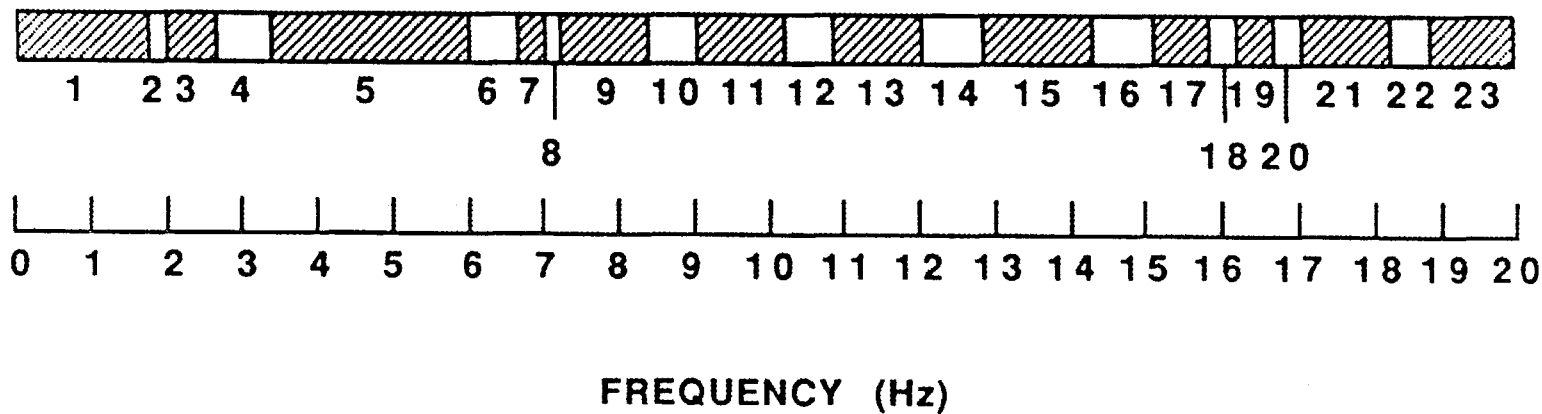


Fig. 4.1. Frequency intervals used to calculate rms² values.

Table 4.1. PSD frequency intervals

Interval number	Lower frequency boundary (Hz)	Upper frequency boundary (Hz)
1	0.10	1.70
2	1.70	2.00
3	2.00	2.70
4	2.70	3.30
5	3.30	6.00
6	6.00	6.70
7	6.70	7.00
8	7.00	7.20
9	7.20	8.30
10	8.30	9.00
11	9.00	10.10
12	10.10	0.90
13	10.90	12.00
14	12.00	12.80
15	12.80	14.30
16	14.30	15.10
17	15.10	15.80
18	15.80	16.10
19	16.10	16.70
20	16.70	17.00
21	17.00	18.05
22	18.05	18.85
23	18.85	20.00
24	0.10	20.00

^aLower frequency limit of analysis.

^bThe 11 frequency bands defined by using PSD peak frequencies.

Table 4.2. Tables and columns in FFTF noise data base

Table name	Column number	Column name	Column type ^a
MEASUREMENT	1	MEASUREMENT_KEY	Number(5)
	2	FILE_KEY	Number(4)
	3	BLOCKSIZE	Number(5)
	4	NUMBER_OF_BLOCKS	Number(5)
	5	AA_FILTER	Number(5)
	6	SAMPLING_RATE	Number(9)
	7	START_DATE	Date(8)
	8	START_TIME	Character(8)
	9	END_DATE	Date(8)
	10	END_TIME	Character(8)
PSD	1	INTERVAL_KEY	Number(2)
	2	MEASUREMENT_KEY	Number(5)
	3	PATCH_KEY	Number(4)
	4	PEAK_FREQUENCY	Number(10)
	5	PEAK_AMPLITUDE	Number(10)
	6	RMS	Number(10)
DCVAL	1	MEASUREMENT_KEY	Number(5)
	2	PATCH_KEY	Number(5)
	3	STARTING_VALUE	Number(10)
	4	ENDING_VALUE	Number(10)
FREQ_INTERVAL	1	INTERVAL_KEY	Number(2)
	2	LOWER_BOUNDARY	Number(5)
	3	UPPER_BOUNDARY	Number(5)
PATCH	1	PATCH_KEY	Number(5)
	2	PATCH_ID	Character(35)
	3	UNITS	Character(30)
DATAFILE	1	FILE_KEY	Number(4)
	2	FILENAME	Character(35)
	3	VOLUME_I	Character(35)

Table 4.2. (continued)

Table name	Column number	Column name	Column type ^a
SIGNAL	1	SIGNAL_KEY	Number(4)
	2	MEASUREMENT_KEY	Number(5)
	3	CHANNEL_NUMBER	Number(4)
	4	PATCH_KEY	Number(5)
	5	AD_MODE	Number(4)
	6	AMP_GAIN	Number(4)

^aOracle uses three data types: number, character, and date. The number in parentheses specifies the length of the data in each column.

The use of index columns is not limited to relating entries in two tables with a common index column. Information in two tables with no common index columns may be related by using a third table with an index column common to each of the other tables. For example, the DATAFILE table may be related to the PSD table, even though neither table has any common index columns, by using index columns from the MEASUREMENT table. The index column "FILE_KEY" is common to both the MEASUREMENT and DATAFILE tables, and the index column "MEASUREMENT_KEY" is common to both the PSD and MEASUREMENT tables. Rows in the DATAFILE table and PSD table are related if the values in the column "FILE_KEY" are equal in both the DATAFILE and MEASUREMENT table and if the values in the column "MEASUREMENT_KEY" are equal in both the PSD and MEASUREMENT tables. A block diagram showing the interrelation between FFTF data base tables is shown in Fig 4.2.

Columns are organized into tables to group similar information. The MEASUREMENT table contains documentation information concerning each ANSDS data set. The PSD table contains the amplitude and frequency of PSD peaks as well as the rms² values for the 24 frequency intervals. The DCVAL table contains the dc value of the reactor states, converted to engineering units, measured at the beginning and the end of the collection of each data set. The FREQ_INTERVAL table identifies each frequency interval with a unique index number. The PATCH table identifies each signal name with its patch panel number ("PATCH_KEY"). The DATAFILE table identifies each ANSDS data file with its identification number ("FILE_KEY"). The SIGNAL table contains documentation information for each PSD.

Several examples illustrating the capabilities of the data base are presented in Appendix A.

ORNL-DWG 88-8739

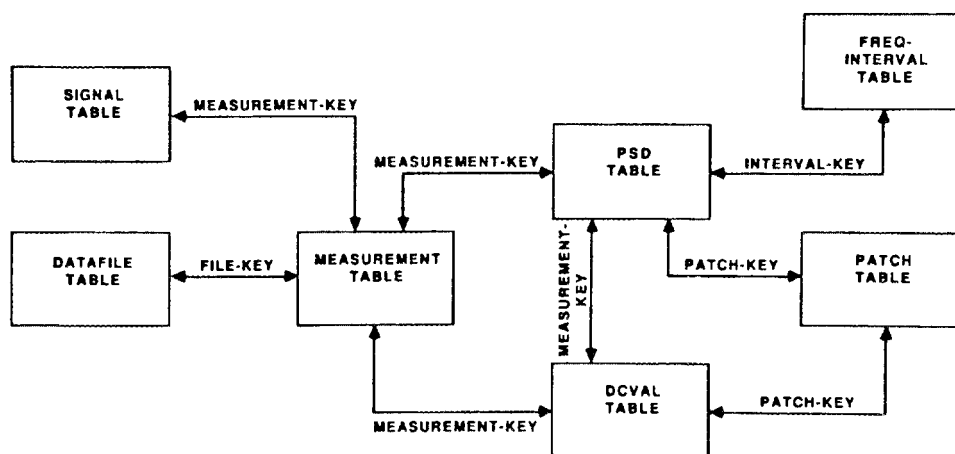


Fig. 4.2. FFIF data base tables and index columns used to relate data in different tables.

5. INTERPRETATION OF DATA

5.1 SIGNAL BACKGROUND

Optimum results are obtained from a noise data collection system if its special requirements are met during plant design or if sufficient backfitting is performed during system installation, because dedicated low-noise cables from the transducers with optimally located preamplifiers are needed to minimize signal contamination. This ideal situation was not possible at the FFTF, as indicated by the signal transmission shown in Fig. 2.3. A special data analysis research challenge exists here: separating out background artifacts from the physical phenomena originating in the reactor.

Obvious background artifacts from 60-Hz signal contamination and its harmonics are found, especially in the nonneutron signals that, unlike the neutron signals, do not have a 20-Hz low-pass filter. Another obvious background effect is signal contamination from the plant's 10-Hz data acquisition equipment. Figures 5.1 and 5.2 show examples of these artifacts and how meaningful physical information also present in the signal can be extracted despite these adverse circumstances. Besides the pump effects identified in Fig. 5.2, correlations of temperature and neutron signals at low frequencies have been seen using signals similar to that shown in Fig. 5.1 and will be discussed below.

Considerable effort is needed to identify background effects present in the noise. It was necessary to employ a variety of phenomena separation techniques—more so than in other noise analyses projects that have the distinct advantages of a more favorable signal transmission environment and continuous manning by a specialist for on-the-spot quality assurance. Special measures in FFTF noise analyses involve ongoing applications of the following:

- Performing special tests at the site with known signals and transmission paths. Noise generator calibrations were done in 1983 in setting up the system and again in 1984.
- Taking data at times when operating conditions and/or signal collection configurations differ significantly from normal. Examples include zero-power operations and disconnection or loss of sensor signals, such as during maintenance and surveillance.
- Looking for coherences between substantially different signals that would be unlikely to be artifacts.
- Using variety in analyses options. Examples include Nyquist frequency changes, amplifier gain changes, off-line analysis of tapes vs the usual on-line analysis on disk, etc.
- Examining absolute magnitudes of spectral regions and determining to what extent, if any, operating conditions influence these.

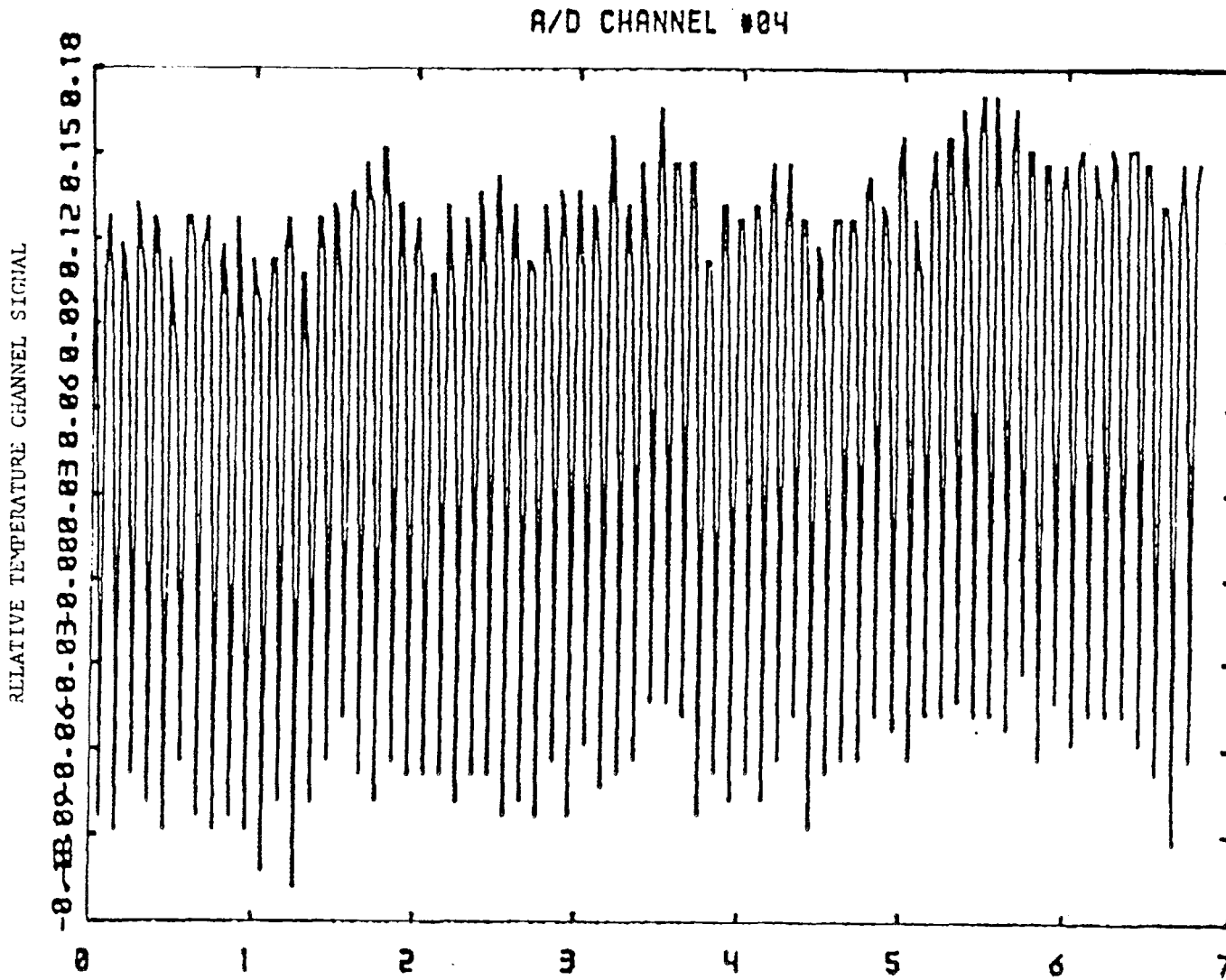


Fig. 5.1. Display of the loop 1 cold leg temperature channel in December 1985 at full power, showing how an asymmetrical 10-Hz signal from plant data acquisition equipment is superimposed on a random temperature fluctuation signal.

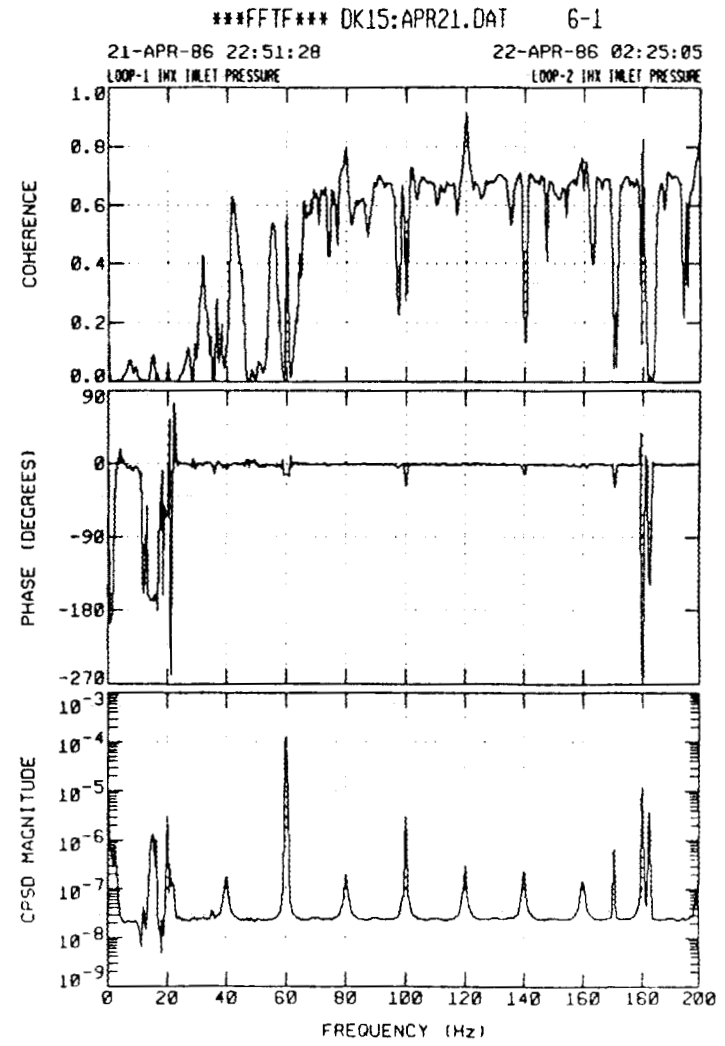
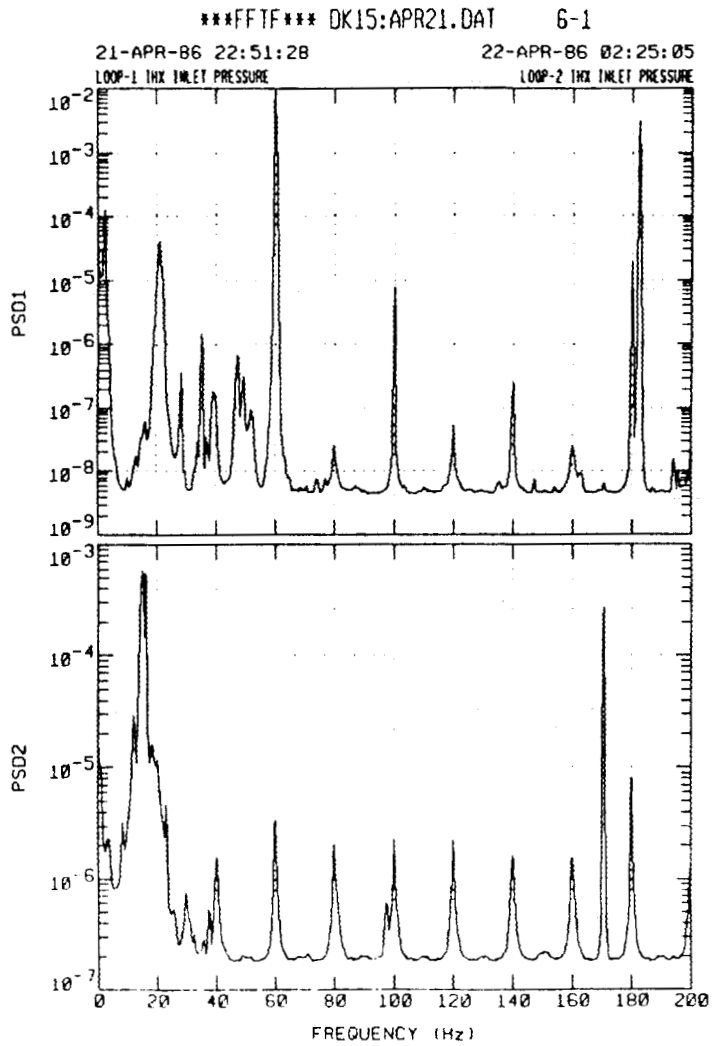


Fig. 5.2. Loop 1 and loop 2 pressures at full power and full flow, showing line frequency artifacts (including aliases) as well as real phenomena from the pumps' 16-Hz rotational frequency and 6 times this as the blade-passing frequency.

- Using available knowledge about potential noise sources, both of an artifactual and a physical nature, and determining how operating conditions influence these.

Regarding the first of these, a white-noise generator was connected directly to the input of the analysis system amplifiers. The absence of spurious peaks, etc., in this test indicated that the analyzing equipment does not have detectable contamination sources.

As a specific example of the application of artifact detection techniques, the following list summarizes information gathered about the characteristics of a persisting resonance at 14.8 Hz. It is seen in all spectra with a Nyquist frequency of 30 Hz except on rare occasions when other phenomena mask it:

- Prior to 1986, slightly lower Nyquist frequencies were used and this peak was never seen.
- It is not seen when Nyquist frequencies of 50 and 100 Hz are used. A 45.2-Hz peak appears in these spectra, suggesting that 14.8 Hz is an alias of this peak in 30-Hz analysis (though an antialiasing filter should prevent this occurrence).

The magnitude in all six neutron detectors is nearly the same no matter what the power (i.e., whether zero or 100%) when background is subtracted from the 14.8-Hz peak. It is found that:

- The product of the peak PSD and analyzer resolution (i.e., reciprocal of block length) for all six is always about $6 \times 10^{-9} \text{ V}^2$.
- The largest difference found (on February 13, 1986) was when the low-level flux monitor 1 (LLFM-1) peak was only two-thirds as large as the other two LLFMs.
- The magnitude is not affected by the closer locations of the LLFMs to the core at very low and zero powers.

Coherence is good among all detectors, usually above 0.5, unless another phenomenon comparable in magnitude appears in this frequency region. There is never coherence with process sensors not having this peak. High-resolution analysis shows that this peak is narrower than 0.06 Hz, indicating an oscillatory origin not typical of mechanical vibrations, which normally have much larger widths. There was also a peak at 29.6 Hz in 1986, with a magnitude half that of the 14.8-Hz peak, suggesting that it is a harmonic.

Interference, such as may be due to a common source, was seen on two occasions:

- with a peak at 16.5 Hz in compensated ion chamber 2 (CIC-2) and
- with a peak in LLFM-3 quite close to and much larger than that at 14.8 Hz.

From the combination of such evidence, it may be possible to reach a conclusion about whether an effect is a background artifact or real. In the case of 14.8 Hz, it is currently believed to be background, though for certainty a confirmatory knowledge of the specific source is still needed.

5.2 CONTROL ROD NOISE

The dominant source of neutron noise at low frequencies, discovered in early work,³⁻⁵ is the lateral motion of control rods within the clearances of their hexagonal ducts. This phenomenon has been the subject of ORNL data analysis^{10,11} by which it was found possible to understand and quantify it quite precisely.

Figure 5.3 shows how low-frequency noise is related to control rod position for a bank of six normal FFTF rods. The abscissa expresses the control rod position as relative reactivity worth. The ordinate, the square root of the integral of the normalized power spectral density (NPSD = PSD divided by dc value squared) below 5 Hz, is dominated by contributions below 1 Hz. With an all-rods-out background removed, it is called here a partial fractional rms. The linearity is consistent with a model of fractional power fluctuations, being proportional to the reactivity fluctuations of this flow-excited laterally fluctuating bank of rods. Table 1.1 shows the rod configurations used in various fuel cycles. In the model developed,¹⁰ it was assumed that all six rods vibrate randomly with respect to each other. Thus their contributions to the PSD would be additive, though unique for each rod type and core location. The final result of this model is the following equation for noise at the beginning of each fuel cycle:

$$\begin{aligned} \text{partial fractional rms in 0.025- to 5-Hz range} = \\ 0.01 * (0.0025n_F + 0.07n_2 + 0.02n_{1A} + 0.1n_{1B})^{1/2} \end{aligned} \quad (5.1)$$

Here n_i is the number of a type of rod present among the six: F designates normal FFTF rods; and 1A, 1B, and 2 are ADVABs. The coefficients were determined by using data⁵ from cycle 6 when different rod types were individually inserted. Equation 5.1 was found to fit noise from cycles 2 through 6 as well as to accurately predict cycle 7 noise, thus verifying its validity.

Besides the rod type that identifies variables in this equation, the core location is also significant. This was found in cycle 9 (by L. R. Campbell of the Westinghouse Hanford Engineering Development Laboratory in February 1987) in which control positions were interchanged (see Table 1.1). Thus, position as well as type would be subscripts in the ultimate form of this equation.

Spectral behavior for different neutron detectors in different fuel cycles is shown in Figs. 5.4 and 5.5. It can be seen that below 5 Hz the only persistent characteristic is a resonance at 0.3 Hz. In this frequency range, all neutron detectors are in phase, have good coherence, and have noise magnitudes proportional to rod-inserted reactivities. It is quite reasonable to hypothesize that this resonance is due to control rod vibration. Possibly supporting this theory is the finding in hydraulic core mockup tests¹² of a 0.25-Hz pendular oscillation for the FFTF control rods.

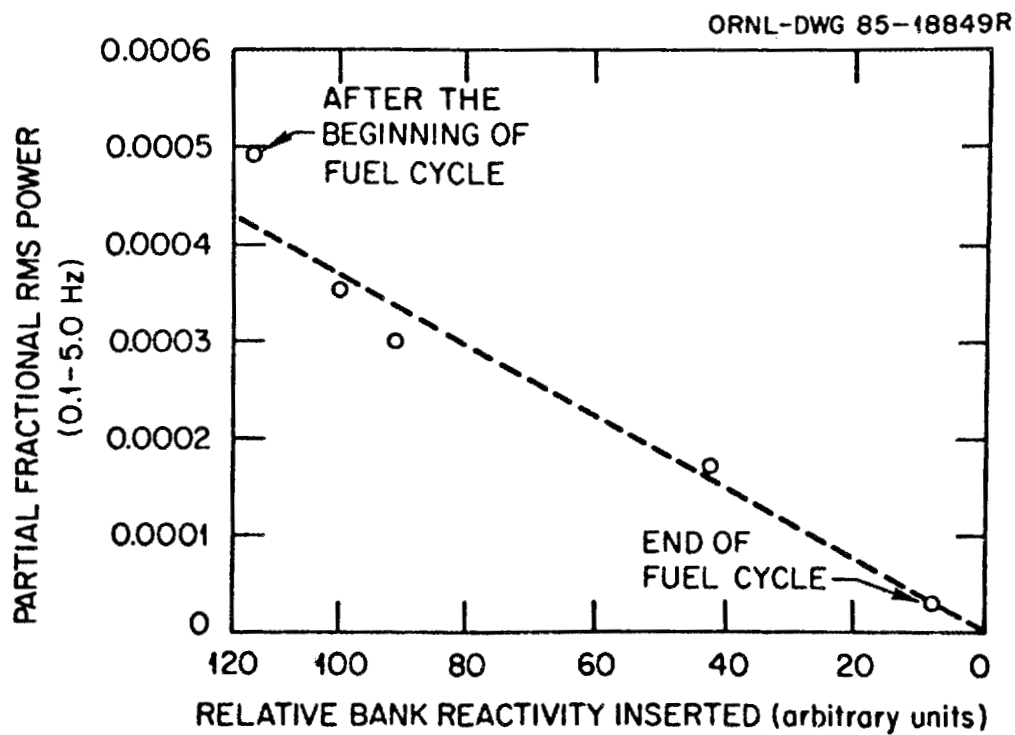


Fig. 5.3. The RMS neutron noise due to control rod fluctuation plotted against the relative worth of the inserted bank during the first fuel cycle. A background rms of 0.000195 (found with all rods out) is removed from all data points before plotting.

PLOT FILE---PSDTA03.D01

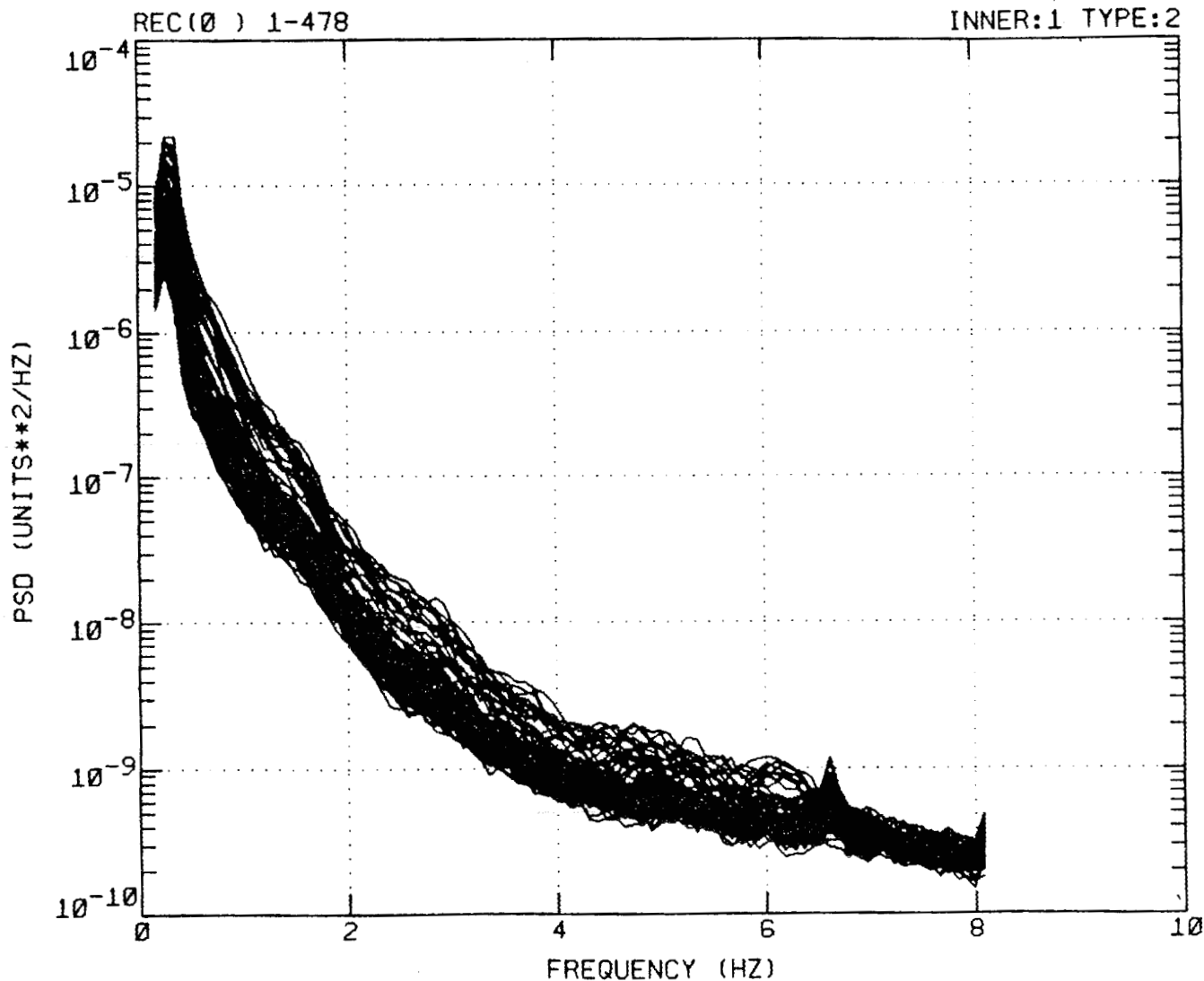


Fig. 5.4. Spectra of LLFM-1 at full power and flow during fuel cycle 5. The band is due to the control rods, responsible for this noise, being withdrawn throughout the entire fuel cycle.

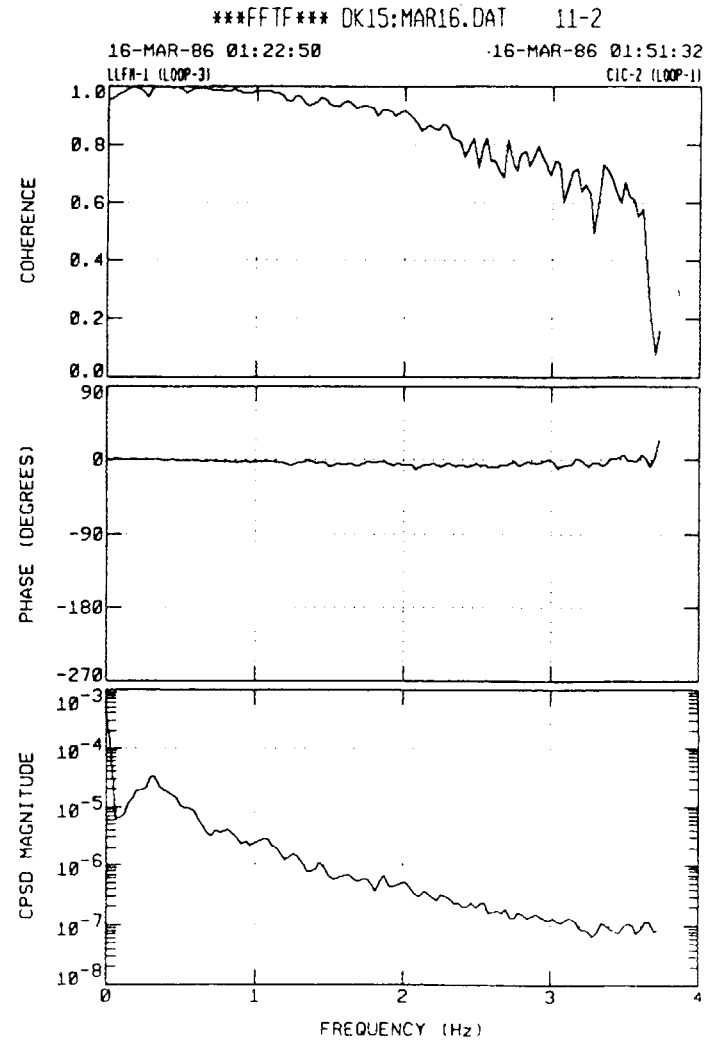
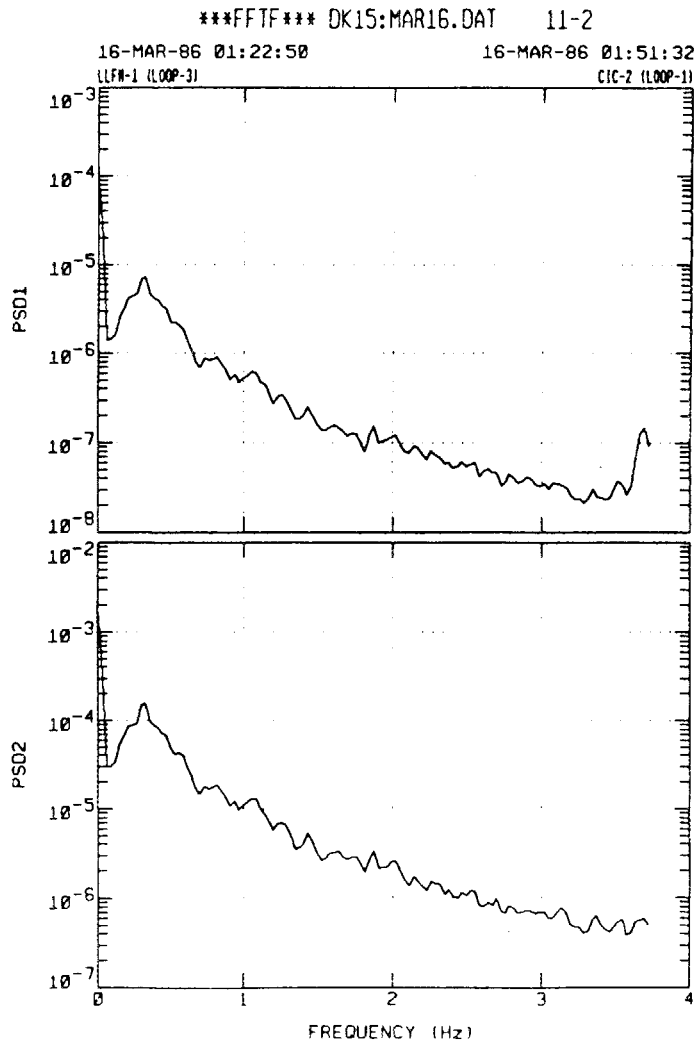


Fig. 5.5. Spectra of neutron detectors at full power and flow during cycle 8.

5.3 FLOW RESONANCE AT 0.06 Hz

In cycle 8, where flow was one of the signals analyzed, it was found that a 0.06-Hz peak in the flow was coherent with neutron signals, as illustrated in Fig. 5.6. Coherence with pressure in loop 1, seen in Fig. 5.7, suggests that there are coolant fluctuations at this frequency. The mechanism (examples being in the pump phenomena discussion below) by which a neutron detector can sense these is yet to be established. Neither has the origin of this peak been found.

5.4 TEMPERATURE REACTIVITY NOISE

Because of the poor quality of the temperature signals (see Fig. 5.1), only limited temperature data collection has been performed. This has been fruitful, however (as in the December 1985 data), when the contamination does not overload amplifiers at the gains required to detect coolant temperature fluctuations.

Hot and cold legs show coherence below 0.02 Hz, which might be presumed to be due to influences from the secondary system that slowly change primary temperatures. Also, at a broad resonance at 0.25 Hz, LLFM and loop temperatures are consistently coherent, with a 180° phase relationship. The NPSD of the neutron signals is always approximately 10^{-8} here. No quantitative model for these effects exists yet. However, magnitudes of the NPSD and temperature fluctuations are in the range that temperature inducing a reactivity and/or power inducing a temperature would quantitatively provide explanations.

5.5 REACTIVITY RESONANCE AT 6.6 Hz

In cycles 3 and 5, a resonance at 6.6 Hz was consistently observed. It was in phase and had exactly the same magnitude among all neutron detectors. Its NSPD—about twice that of the random control rod motion effect—changes during a fuel cycle in the same manner as the wideband noise due to control rod fluctuations. Additional characteristics are:

- A harmonic at 19.8 Hz is also seen, with its NPSD about a decade lower than that of the 6.6-Hz resonance. This would be compatible with a symmetrical square wave oscillation.
- In recent fuel cycles, the NPSD of neutron signals due to the wideband control rod noise may have been too large to observe this phenomenon, which would barely exceed background.
- All six neutron signals show coherence with a vertical motion accelerometer on the vessel (Fig. 5.8 is typical).
- Calculations have shown a 6.3-Hz resonance in the control rod driveline, and scale model tests have shown impacting from flow excitation.¹³

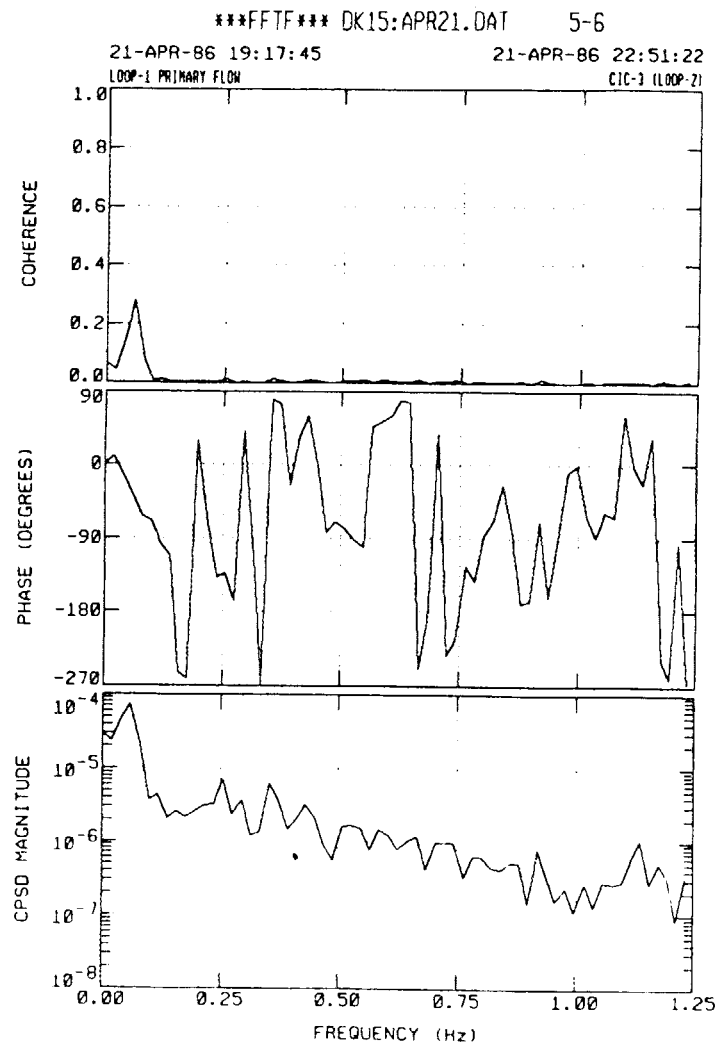
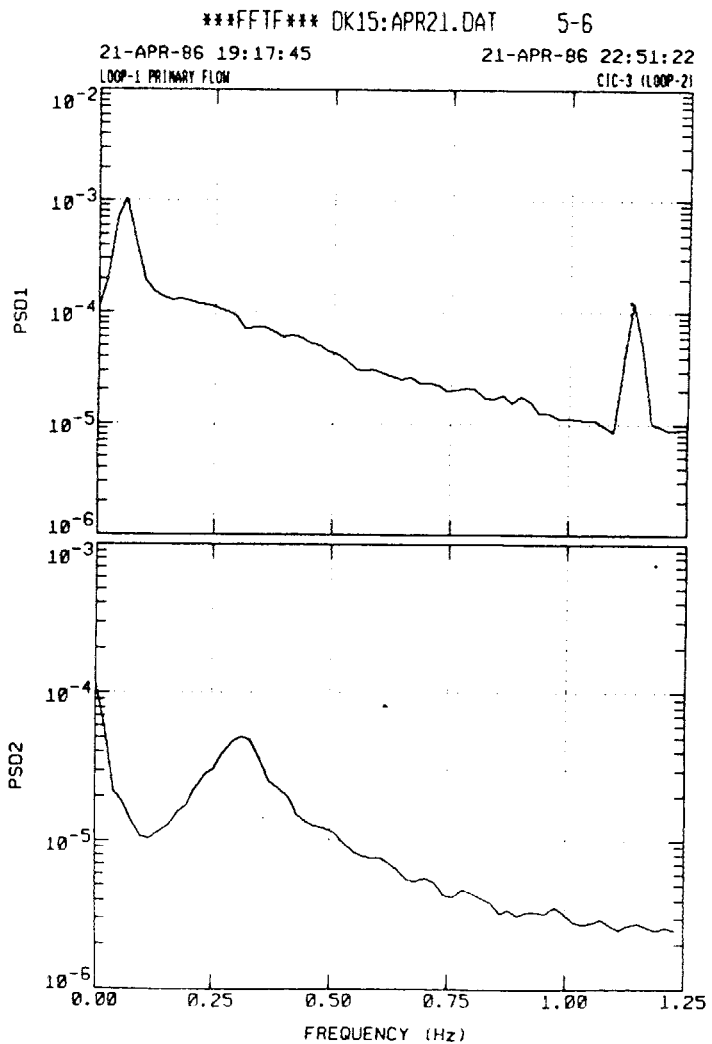


Fig. 5.6. Low-frequency spectra of flow and neutron detectors at full power and full flow, showing their coherence at the flow's 0.06-Hz resonance.

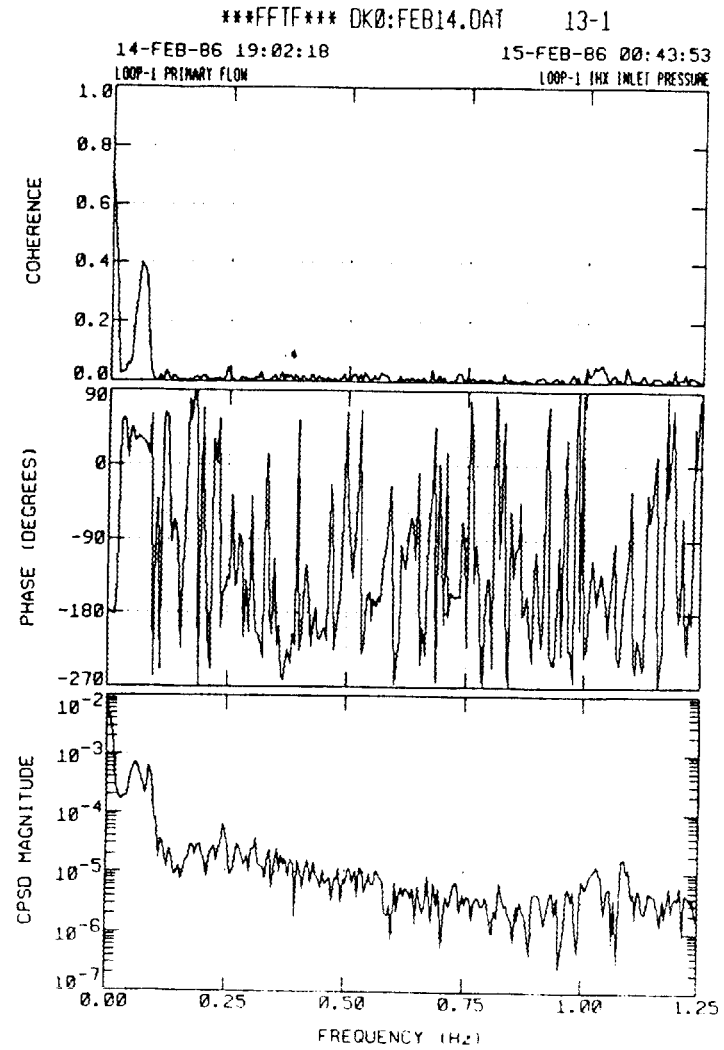
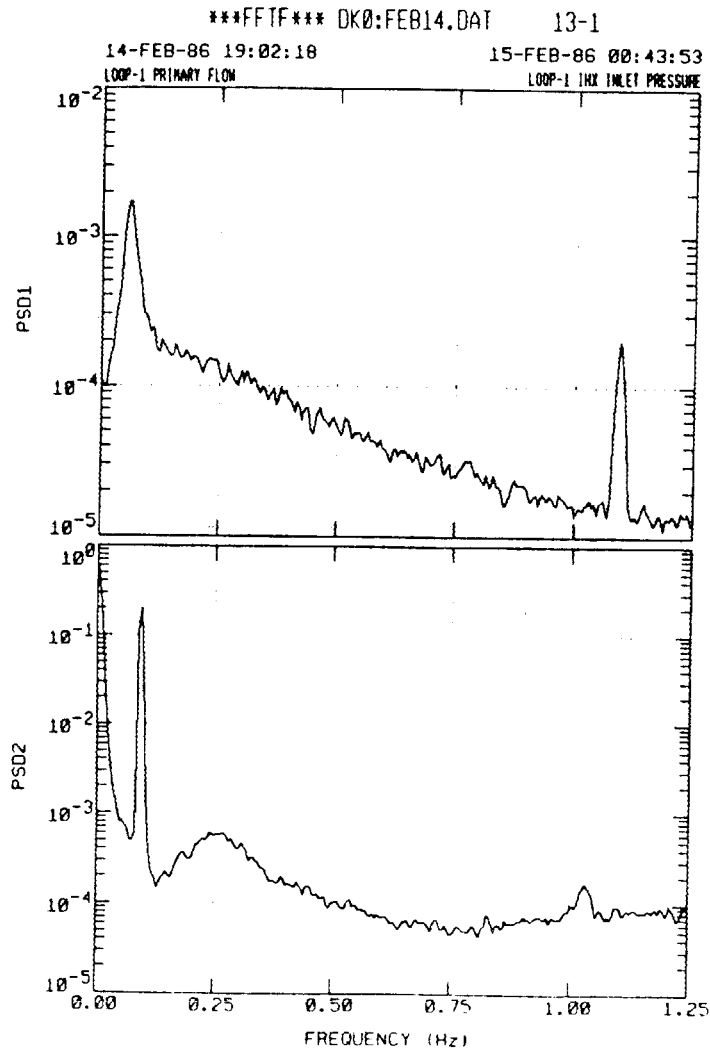


Fig. 5.7. Low-frequency spectra of loop 1 flow and pressure at full power and full flow, showing their coherence at the 0.06-Hz resonance.

FFTF PRELIMINARY ANALYSIS

* BLOCKS 198
DELF 7.80×10^{-2}
BLK-SIZE 512
OVERLAP 256

B-LLFM2
H-VESSEL VERT ACC

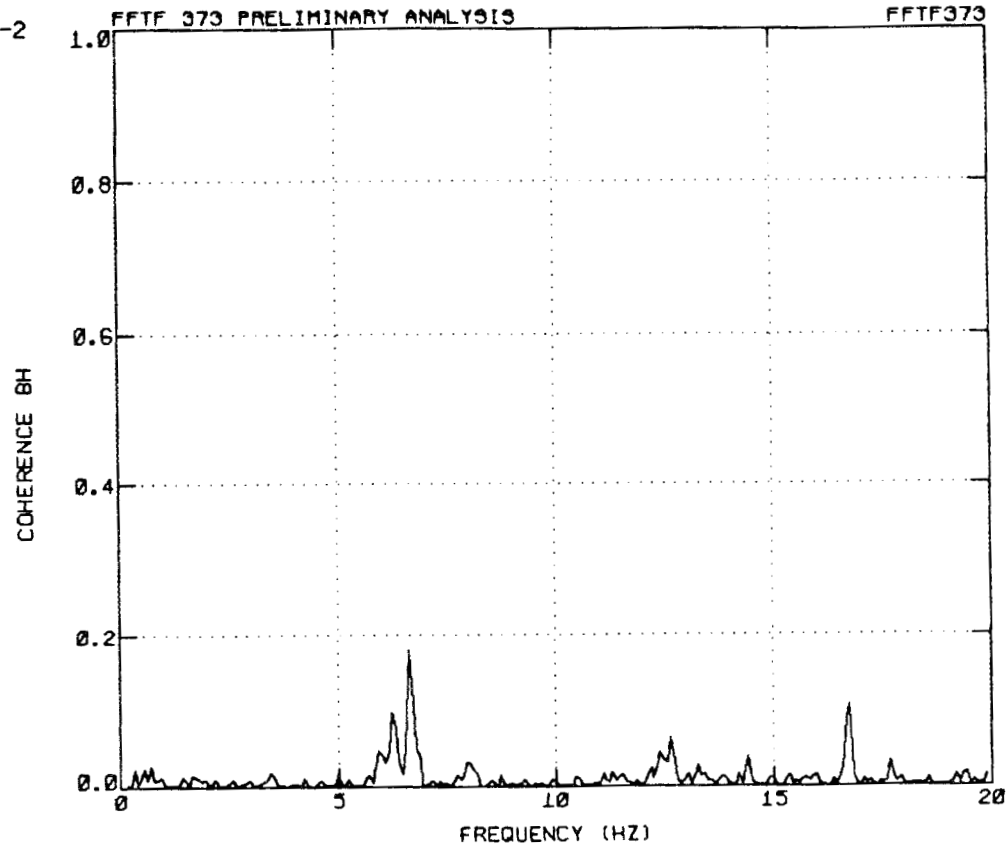


Fig. 5.8. Coherence between an in-vessel fission chamber LLFM-2 and a vessel accelerometer at full power and flow in August 1983. The control rod reactivity effect at 6.6 Hz is clearly seen; the second peak at 6.25 Hz is a harmonic of a strong accelerometer (but not neutron) peak at 1.25 Hz. The resonance at 16.7 Hz is evident and is believed to be due to the pump imbalance frequency at that particular time.

Evidence suggests the hypothesis of a lateral control rod vibration at this frequency with nonlinearities caused by amplitude limitations. As indicated in Fig. 5.8, there is also a possibility of excitation in this frequency region by a fifth harmonic of a strong 1.25-Hz resonance.

5.6 INTERFERING RESONANCES

A persistent phenomenon in the neutron signals over all the fuel cycles in the vicinity of 10 Hz was found to have the following characteristics:

- A resonant peak is seen with slightly different frequencies in various fuel cycles. It was first identified in cycle 1 as being in the 6- to 8-Hz range.¹⁴ During cycle 3 it changed from 9.8 to 12 Hz. It was constant at 11.5 Hz throughout cycle 8. The 12.9-Hz in cycle 9 is the highest value seen.
- Different detectors show different resonant frequencies and amplitudes, as illustrated in Fig. 5.9. LLFMs show the phenomenon best. However, for a given detector the product of the peak PSD and analysis resolution does not usually vary more than a factor of 2, even over many fuel cycles: 5×10^{-8} , 10^{-9} , and 10^{-7} V^2 for LLFM-1, LLFM-2, and LLFM-3 respectively.
- High-resolution spectra show interference patterns between two related peaks, as in Figs. 5.10 and 5.11. These spectra may have an in-phase or out-of-phase pattern. Interference patterns observed in cycle 1 (ref. 14) are still present.
- Control rod configuration and powers over 50% have no influence over the peak PSD.

A mathematical model accounting for this behavior¹⁰ assumes that slightly different transfer functions H_i are associated with different signals or physical regions, but all are excited by a common source S .

For the i th resonant frequency f_i with a damping ratio of z , the transfer function of a second-order system is

$$H_i = [1 - (f/f_i)^2 + j^2 z_i (f/f_i)]^{-1} \quad (5.2)$$

Signals of the two interfering detectors are constructed from contributions from two transfer functions and a background source S' :

$$X_1 = (a_{11}H_1 + a_{12}H_2)S + S' \quad (5.3a)$$

$$X_2 = (a_{21}H_1 + a_{22}H_2)S + S' \quad (5.3b)$$

Using best fits for its empirical apportioning parameters a_{ij} , resonance parameters, and ratio of sources, the calculated results from this model are shown in Figs. 5.10 and 5.11. With cross-coupling a_{ij} 's (i, j) taken as zero, a_{11} and a_{22} have the same sign for the

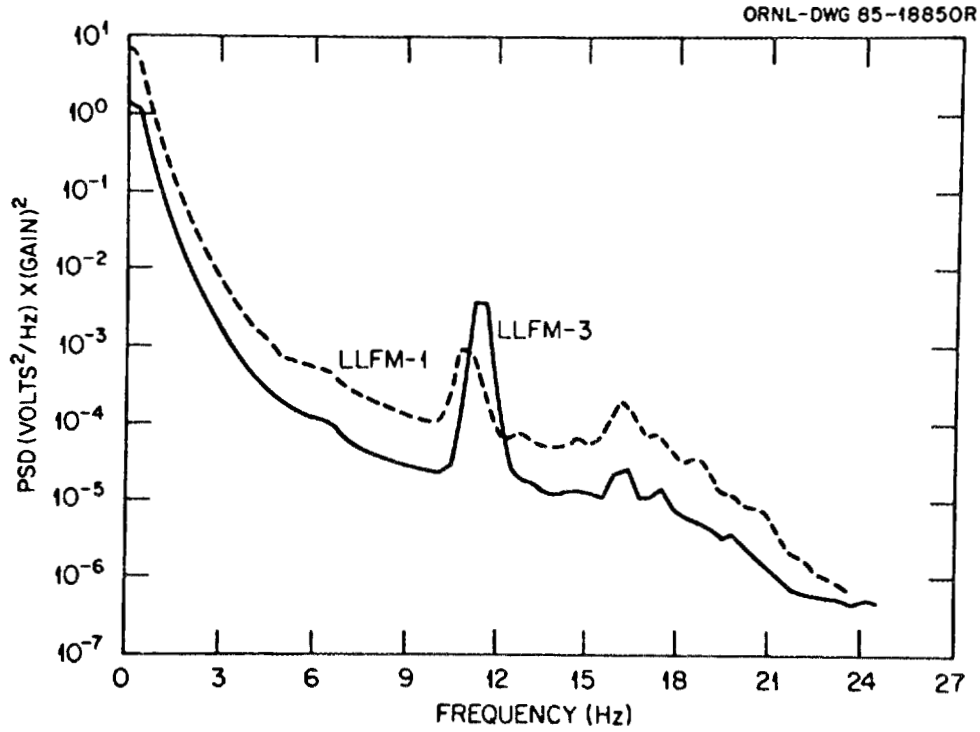


Fig. 5.9. Spectra taken in June 1984, showing how two LLFMs detect slightly different resonant frequencies (~11 Hz). With gain = 128 and 256 for LLFM-3 and LLFM-1, respectively, the ~11-Hz peak is much stronger in the former. The peak at 16 Hz due to the primary pumps is also seen here.

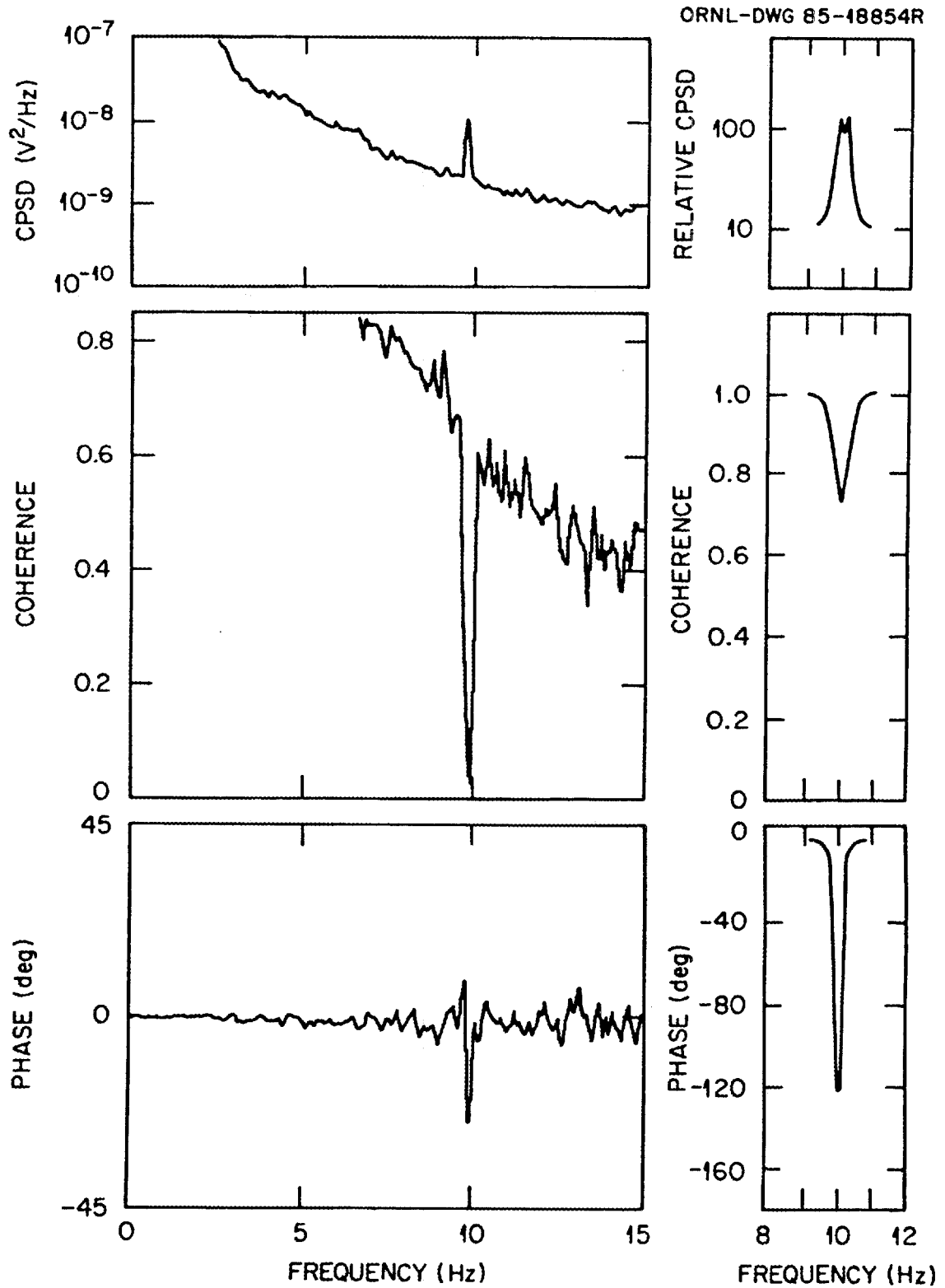


Fig. 5.10. LLFM-1 and LLFM-2 in August 1983 exhibiting in-phase interference of two closely spaced resonances near 10 Hz. Calculations from a physical model (shown on the right) exhibit the same features as the data.

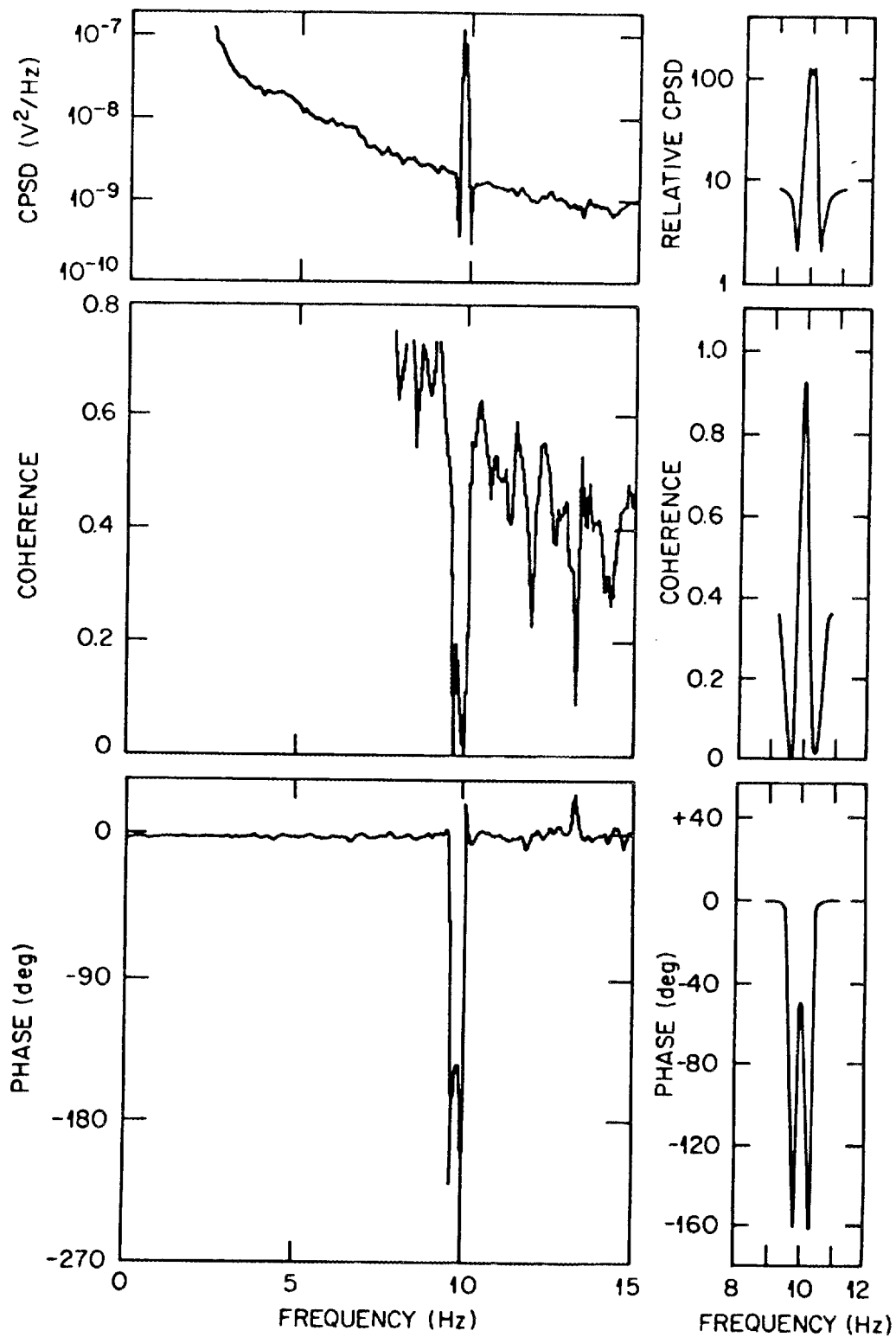


Fig. 5.11. LLFM-1 and LLFM-3 in August 1983 exhibiting out-of-phase interference of two closely spaced resonances near 10 Hz. Calculations from a physical model (shown on the right) exhibit the same features as the data.

pair of detectors in Fig. 5.10 and the opposite sign for a different pair of detectors in Fig. 5.11. It can be seen that the mathematical basis for the phenomenon is well identified. It remains for additional investigations to determine the physical basis for this interfering double resonance. In particular, it must be ascertained whether it is reactor associated or is an artifact. One speculation is that different mechanical structures located in different regions are being shaken in common. Here one might note core accelerometer results during reactor commissioning that gave frequencies in the neighborhood of 10 Hz (varying from time to time) and whose horizontal and vertical resonances differed slightly.¹⁴

5.7 PUMP PHENOMENA

Extensive manifestations of a major noise source, the primary pumps, have been found in the noise of most signals. For example, Figs. 5.2, 5.8, and 5.9 show typical pump effects at both rotational and blade-passing frequencies. The specific ways in which the primary pumps are seen in signal noise are as follows:

- A fundamental frequency associated with pump imbalance appears in all neutron detectors, the loop 2 pressure sensor, loop 1 and 2 pressure sensor coherence, and loop 2 pressure and neutron detector coherence. It is easier to see at higher powers in neutron sensors. Accelerometers also show this peak; there is coherence with all six neutron detectors, with Fig. 5.8 being typical.
- A harmonic at twice the rotational frequency appears in the loop 2 pressure.
- With six impeller blades, 6 X rotational frequency is a peak in loop 2's pressure.
- The relationship between the observed fundamental frequency peak and the total flow of three loops is a precise proportionality: 0.41 Hz/K-gpm. This is same factor obtained from control room pump speed and flow instruments.
- Slight variations of speed between loops have the effect of giving a width of typically 0.1 Hz or less to the fundamental's peak at half maximum. High-resolution analyses can observe individual pump peaks.

One likely mechanism by which pump phenomena are transmitted to the pressure sensors is pressure pulses in the sodium, especially at the blade-passing frequency. The mechanism by which neutron detectors observe pump frequency is yet to be established. Possibilities are core vibration, detector vibration, coolant pressure-density effects, and pickup by cables.

5.8 OTHER RESONANCES

An application of a peak detection algorithm to a variety of control rod configurations in cycle 9 resulted in finding a number of resonances yet to be explained.¹¹ The in-vessel neutron detectors consistently showed many more peaks than the ex-vessel

compensated ion chambers (which showed only the pump rotational frequency): 7.5, 11, 21.6, 23.8, 25.3, and 26.8 Hz were seen in all three LLFMs in analyses up to 30 Hz.

In cycles 7 and 8, using visual identification of peaks, substantial numbers of resonances beyond these persistent ones were found. In these analyses the following were varied: transducer type, month in the fuel cycle, power, flow, and Nyquist frequency. The data base structure already described was found necessary to compile the rather voluminous information of observed resonances and associated conditions. Because of the variety of conditions available, this data base could be especially attractive for understanding additional phenomena.

6. FUTURE POSSIBILITIES

Future activities envisioned in noise analysis of the FFTF fall in the areas of improved hardware/software and better understanding of the phenomena, with a view toward practical applications. The former involves a changeover of the computer used at the site and software enhancements to make possible more versatile data collection activities. The latter involves completing the partial understandings discussed in the Sect. 5, finding new insights, and putting selected understandings to use.

Anticipated directions that could be taken toward obtaining insights into the noise phenomena are examination of past data and planning, taking, and analyzing future data. As seen in Tables 3.1 and 3.2, a wealth of information already exists. The variety of conditions represented by these data is not likely to be available in future data for several years. On the other hand, additional data are needed to answer questions arising during the process of obtaining insights. A complete understanding of a phenomenon is often the result of an interactive approach to analysis and data collection.

A type of interaction between the analyst and the data that could be useful in this work is making extensive use of the FFTF noise data base. This likely could involve a dynamic data base, that is, one with new tables constructed from selected features in the spectra.

Identifications of noise discussed in Sect. 5 were often incomplete. Usually missing were the physical nature of the resonance source. If these are found by further efforts, then possibilities might exist for monitoring applications related to that physical source. Except for control rod noise, a complete quantitative model does not exist for any phenomenon. Modeling would be the ultimate in understanding, an accomplishment not unusual in pressurized water reactor (PWR) noise applications.

By analogy with practical applications of noise analysis in other reactors and noting the effects already observed in the FFTF, a list of representative monitoring possibilities can be compiled. These would be areas in which something of practical value to operations would result from noise analysis of a specific phenomenon. The following list is somewhat speculative in that it depends on the outcome of further research. However, it is not totally speculative because all of its items have been accomplished in closely related systems on PWRs. The first item is already an operational tool at the FFTF as an outcome of substantial research effort.

- If a configuration of types of control rod is planned for a future fuel cycle, expected noise can be predicted and compared to operational limitations on what can be tolerated.
- When spectra and cross-spectra involving a particular transducer depart from norms for a particular operating condition, there can be an early alert of a system abnormality if other transducers confirm this or an early warning of a transducer malfunction. The integration of continuous instrumentation surveillance with periodic traditional surveillance tests can possibly lead to some relaxation in the latter and/or a still better program.

- As a supplement to direct mechanical motion monitoring of pumps, the same resonances can be monitored in process instrumentation. If there is a pump problem, additional confirmatory data probably would be welcomed.
- Structural vibrations of the core and its immediate surroundings could, if specifically identified, be continuously monitored to obtain early warning of problems. Such a program would be integrated into and enhance other mechanical integrity surveillance programs.
- An understood relationship between neutron and temperature noise could permit continuous monitoring for early warnings of changes in the temperature coefficient of reactivity that might be due to system anomalies. This particular noise monitoring was implemented on the Fermi-1 upon restart after its meltdown from a progressing temperature anomaly due to a flow blockage.

7. ACKNOWLEDGMENTS

In the years 1983 through 1986, the data for this program were taken by J. A. Mullens and W. T. King of ORNL. Moreover, they instituted extensive software developments in the automatic data collection system. Information and hardware assistance from L. R. Campbell of Westinghouse-Hanford was invaluable throughout our entire program.

8. REFERENCES

1. J. A. Mullens, J. A. Thie, and L. R. Campbell, "On-line Noise Monitoring at the Fast Flux Test Facility," Specialists Meeting on Reactor Noise IV, Dijon, France (1984).
2. C. P. Cabell, *A Summary Description of the Fast Flux Test Facility*, HEDL-400, Westinghouse, Hanford, Wash., December 1980.
3. R. B. Bennett, *ATP Neutron Noise Data Report*, HEDL-TC-2394, Westinghouse, Hanford, Wash., 1981.
4. S. K. Varnes et al., "Predictions of Power Fluctuations Due to Control Rod Vibration," *Trans. Am. Nucl. Soc.* 46, 742 (1984).
5. L. R. Campbell, *Cycle 6 Power Fluctuation Investigation*, Westinghouse Hanford Memo (July 1985).
6. C. M. Smith, *A Description of the Hardware and Software of the Power Spectral Density Recognition (PSDREC) Continuous On-Line Reactor Surveillance System*, Vol. 1, NUREG/CR-3439, V1, U.S. Nuclear Regulatory Commission, 1983.
7. C. M. Smith and R. C. Gonzalez, "Long-Term Automated Surveillance of a Commercial Nuclear Power Plant," Specialists Meeting on Reactor Noise IV, Dijon, France (1984).
8. *Oracle Overview and Introduction to SQL*, 2d ed., Oracle Corp., Belmont, Calif., May 1985.
9. F. J. Sweeney, *Utility Guidelines for Reactor Noise Analysis*, EPRI NP-4970, Electric Power Research Institute, Palo Alto, Calif., February 1987.
10. J. A. Thie, J. A. Mullens, and L. R. Campbell, "Experiences and Results from an Automated Noise Surveillance System of the Fast Flux Test Facility," Proceedings of the 6th Power Plant Dynamics Control and Testing Symposium, The University of Tennessee, Knoxville (August 1986).
11. J. A. Thie, "Fast Flux Facility Noise Data Management," Specialists Meeting on Reactor Noise V, Munich, Germany (1987).
12. K. R. Birney and G. E. Edison, *Final Design Support Document for FFTF Control Rod System, Absorber Assembly, Driveline, and Drive Mechanism*, Vol. 1, FCI-1210, Westinghouse, Hanford, Wash., 1974.

13. J. A. Ryan and L. J. Julyk, *Scale-Model Characterization of Flow-Induced Vibrational Response of FTR Internals: Summary Report*, HEDL-TME 76-1, Westinghouse, Hanford, Wash., 1977.
14. L. Julyk, *Vibration Testing of Reactor Components*, MTER 11-1, Westinghouse, Hanford, Wash., January 1982.



Appendix A

EXAMPLES USING THE FFTF NOISE DATA BASE

Appendix A

EXAMPLES USING THE FFTF NOISE DATA BASE

To illustrate some of the capabilities of the Fast Flux Test Facility (FFTF) data base, this appendix presents several sample searches. The Oracle Data Base Management System uses the Structure Query Language (SQL) to insert, manipulate, and recall values. In addition to search results, each sample search will show the SQL command used to define the search conditions (SQL commands are for the most part self-explanatory). Information describing the SQL query language and Oracle may be found in *Oracle Overview and Introduction to SQL*, 2d ed., Oracle Corp., Belmont, California (May 1984).

EXAMPLE 1

In this example, the square of the root-mean-square (rms^2) value calculated for compensated ion chamber 2 (CIC-2) over the frequency range of 0.1 to 20 Hz and the corresponding date will be selected from data collected between March and September of 1987. Table A.1 shows that the value of PATCH_KEY corresponding to CIC-2 is 23. Table A.2 shows that the value of INTERVAL_KEY specifying the frequency interval from 0.1 to 20 Hz is 24. Table A.3 shows that these data are composed of only normal operating data collected during cycle 9. The data values are stored in the DCVAL table, and the dates are stored in the MEASUREMENT table. This example will show how the MEASUREMENT_KEY index column in the two tables is used to select corresponding information.

The SQL command that will select values that satisfy the above conditions is:

```
1 SELECT TO_CHAR(START_DATE,'DDD')START_DATE,  
2        TO_CHAR(START_DATE,'HH24')START_DATE,  
3        TO_CHAR(START_DATE,'MI')START_DATE,  
4        TO_CHAR(START_DATE,'SS')START_DATE,  
5        TO_CHAR(START_DATE,'YY')START_DATE,RMS  
  
6 FROM MEASUREMENT,PSD  
  
7 WHERE MEASUREMENT.MEASUREMENT_KEY=PSD.MEASUREMENT_KEY  
8        AND  
9        PSD.PATCH_NUMBER=23 AND  
10       PSD.INTERVAL_KEY=24 AND  
11       START_DATE BETWEEN 1-MAR-87 AND 11-SEP-87  
  
11 ORDER BY MEASUREMENT.START_DATE;
```

Table A.1. ANSDS patch panel signals

Patch panel position	Signal name	Engineering units ^a
1	Loop-1 primary flow	K-gpm ^b
2	Loop-2 primary flow	K-gpm
3	Loop-3 primary flow	K-gpm
4	Loop-1 secondary flow	K-gpm
5	Loop-2 secondary flow	K-gpm
6	Loop-3 secondary flow	K-gpm
7	Loop-1 primary hot leg temperature	°F
8	Loop-1 primary cold leg temperature	°F
9	Loop-2 primary hot leg temperature	°F
10	Loop-2 primary cold leg temperature	°F
11	Loop-3 primary hot leg temperature	°F
12	Loop-3 primary cold leg temperature	°F
13	Loop-1 IHX ^c inlet pressure	psi
14	Loop-2 IHX inlet pressure	psi
15	Loop-3 IHX inlet pressure	psi
16	LLFM-1 count rate	volt
17	LLFM-2 count rate	volt
18	LLFM-3 count rate	volt
19	LLFM-1 (loop-3)	volt
20	LLFM-2 (loop-1)	volt
21	LLFM-3 (loop-2)	volt
22	CIC-1 (loop-3)	% full power
23	CIC-2 (loop-1)	% full power
24	CIC-3 (loop-2)	% full power

^aUnits as stored in the Au, FFTF noise data base.

^bK-gpm = 1000 gal/min.

^cIHX = intermediate heat exchanger.

Table A.2. PSD frequency intervals

Interval number	Lower frequency boundary (Hz)	Upper frequency boundary (Hz)
1	0.10 ^a	1.70
2 ^b	1.70	2.00
3	2.00	2.70
4 ^b	2.70	3.30
5	3.30	6.00
6 ^b	6.00	6.70
7	6.70	7.00
8 ^b	7.00	7.20
9	7.20	8.30
10 ^b	8.30	9.00
11	9.00	10.10
12 ^b	10.10	0.90
13	10.90	12.00
14 ^b	12.00	12.80
15	12.80	14.30
16 ^b	14.30	15.10
17	15.10	15.80
18 ^b	15.80	16.10
19	16.10	16.70
20 ^b	16.70	17.00
21	17.00	18.05
22 ^b	18.05	18.85
23	18.85	20.00
24	0.10	20.00

^aLower frequency limit of analysis.

^bThe 11 frequency bands defined by using PSD peak frequencies.

Table A.3. ANSDS data files stored at ORNL

Data disk	File name	Date	Channel number ^a	Analysis number ^b	Conditions ^c
FFTF					
Data 1	DEC19.DAT	12/19/85	2	12	100% power, 100% flow
	FEB07.DAT	2/07/86	5(3), 12(2)	17	65% power, 95% flow
	FEB10.DAT	2/10/86	7(3), 15(2)	22	90% power, 95% flow
	FEB12.DAT	2/12/86	5(3), 3(2)	8	90% power, 95% flow
	FEB13.DAT	2/13/86	3(3), 6(2)	9	100% power, 100% flow
	FEB14.DAT	2/14/86	12(4), 2(2)	14	100% power, 100% flow
	FEB15.DAT	2/15/86	12(4), 2(2)	14	100% power, 100% flow
	FEB16.DAT	2/16/86	12(4), 2(2)	14	100% power, 100% flow
	FEB17.DAT	2/17/86	4	84	100% power, 100% flow
	FEB18.DAT	2/18/86	4	84	65% power, 65% flow
	FEB19.DAT	2/19/86	4	84	65% power, 95% flow
FFTF					
Data 2	FEB20.DAT	2/20/86	4	84	64% power, 78% flow
	FEB21.DAT	2/21/86	4	84	64% power, 95% flow
	FEB22.DAT	2/22/86	4	84	64% power, 67% flow
	FEB23.DAT	2/23/86	4	84	60% power, 100% flow
FFTF					
Data 3	FEB28.DAT	2/28/86	4	84	42% power, 66% flow
	MAR01.DAT	3/01/86	4	84	37% power, 95% flow
	MAR02.DAT	3/02/86	4	84	25% power, 65% flow
	MAR03.DAT	3/03/86	4	84	19% power, 95% flow
FFTF					
Data 4	MAR05.DAT	3/04/86	4	72	24% power, 65% flow
	MAR06.DAT	3/06/86	4	72	24% power, 95% flow
	MAR07.DAT	3/07/86	4	72	37% power, 95% flow
	MAR09.DAT	3/09/86	4	72	15% power, 73% flow
	MAR10.DAT	3/10/86	4	60	9% power, 96% flow
FFTF					
Data 5	DATA3.DAT	1/12/87	4	16	Control rod test
	DATA4.DAT	1/12/87	4	40	Control rod test
	DATA5.DAT	1/13/87	4	40	Control rod test
	DATA6.DAT	1/13/87	4	40	Control rod test
	DATA7.DAT	1/14/87	4	32	Control rod test
	DATA8.DAT	1/14/87	4	20	Control rod test

Table A.3. (continued)

Data disk	File name	Date	Channel number ^a	Analysis number ^b	Conditions ^c
FFTF					
Data 6	MAR24.DAT	3/24/87	4	10	Normal operation
	APR6.DAT	4/06/87	4	10	Normal operation
	APR14.DAT	4/14/87	4	10	Normal operation
	APR20.DAT	4/20/87	4	10	Normal operation
	APR28.DAT	4/28/87	4	10	Normal operation
	MAY4.DAT	5/04/87	4	10	Normal operation
	MAY11.DAT	5/11/87	4	10	Normal operation
	JUN10.DAT	6/10/87	4	10	Normal operation
	JUN15.DAT	6/15/87	4	10	Normal operation
	JUL22.DAT	7/22/87	4	10	Normal operation
	SEPT10.DAT	9/10/87	4	10	Normal operation
	SEP151.DAT	9/15/87	4	32	Control rod test
	SEP152.DAT	9/15/87	4	32	Control rod test
	SEP162.DAT	9/16/87	4	32	Control rod test
	SEP163.DAT	9/16/87	4	32	Control rod test
	SEP171.DAT	9/17/87	4	32	Control rod test
FFTF					
Data 7	OCT7.DAT	10/07/87	4	32	Normal operation
	OCT13.DAT	10/13/87	4	32	Shutdown data
	OCT14.DAT	10/14/87	4	32	Shutdown data
	OCT15.DAT	10/15/87	4	32	Shutdown data
	OCT16.DAT	10/16/87	4	32	Shutdown data
	NOV10.DAT	11/10/87	4	32	Shutdown data
	DEC02.DAT	12/02/87	4	10	Normal operation
	DEC14.DAT	12/14/87	4	10	Normal operation
	DEC21.DAT	12/21/87	4	10	Normal operation
	JAN04.DAT	1/04/88	4	10	Normal operation

^aNumber of data signals for which power spectral densities (PSDs) are calculated. If all data sets in a data file do not calculate PSDs for the same number of signals, the expression A(B),C(D) appears. A(B),C(D) indicates that A data sets calculated PSDs for B signals and C data sets calculated PSDs for D signals.

^bNumber of data sets in the data file.

^cPower and flow values indicate interesting conditions at which data were collected. These conditions, in general, are not constant for all data sets in the data file.

Lines 1 through 4 select the day, hour, minute, and second of the date. Line 5 selects the year and the rms² value. Line 6 specifies that the data are to be selected from the MEASUREMENT and PSD tables. Lines 7 through 10 specify the conditions that must be satisfied by the data selected. The index column "MEASUREMENT_KEY" is used in line 7 to ensure that data values selected from both tables were obtained during the same measurement. Line 11 causes the results to be displayed in chronological order. The results of this search are listed in Table A.4 and plotted in Fig. A.1. Note the similarity of Figs. A.1 and A.2.

EXAMPLE 2

In this example the reactor power, measured by CIC-2, and the value of MEASUREMENT_KEY are selected for data originally stored in the ANSDS data file FEB23.DAT. From Table A.1 the value of PATCH_KEY corresponding to CIC-2 is 23. The SQL command used to perform this search is:

```

1 SELECT DCVAL.MEASUREMENT_KEY,STARTING_VALUE,FILENAME
2 FROM DCVAL,DATAFILE,MEASUREMENT
3 WHERE DATAFILE.FILENAME = 'FEB23.DAT' AND
4   DATAFILE.FILE_KEY=MEASUREMENT.FILE_KEY AND
5   MEASUREMENT.MEASUREMENT_KEY=DCVAL.MEASUREMENT_KEY
   AND
6   DCVAL.PATCH_NUMBER= 23;
```

Line 1 defines the data that will be selected. Line 2 specifies the tables that will be searched. Lines 3 through 6 define the conditions that data values must meet in order to be selected. In this example the MEASUREMENT table is used to select corresponding entries from the DCVAL and DATAFILE tables. The MEASUREMENT and DATAFILE tables each contain the FILE_KEY index column which, in line 4, is used to relate values from these tables. The MEASUREMENT and DCVAL tables each contain the MEASUREMENT_KEY index column which is used in line 5 to relate values from these tables. When both of these conditions are satisfied, the values selected from the DCVAL and DATAFILE tables were measured during the same measurement period. The results of this search are shown in Table A.5.

Table A.4. Example 1 search results

Day	Hour	Minute	Second	Year	Square of root mean square
83	12	44	9	1987	4.928482E-06
83	12	59	8	1987	4.930137E-06
83	13	6	37	1987	5.248427E-06
83	13	21	37	1987	4.747628E-06
83	13	29	6	1987	4.926024E-06
83	13	44	6	1987	5.008209E-06
96	6	6	37	1987	4.344153E-06
96	6	21	37	1987	4.071389E-06
96	6	29	6	1987	3.974529E-06
96	6	44	6	1987	4.071404E-06
96	6	51	36	1987	4.105455E-06
96	7	6	36	1987	4.034257E-06
104	8	23	26	1987	3.890765E-06
104	8	38	25	1987	3.966431E-06
104	8	45	55	1987	3.425924E-06
104	9	0	55	1987	3.842735E-06
104	9	8	25	1987	3.702482E-06
104	9	23	25	1987	3.974857E-06
110	7	20	11	1987	3.524168E-06
110	7	35	10	1987	3.455779E-06
110	7	42	40	1987	3.567820E-06
110	7	57	40	1987	3.885205E-06
110	8	5	10	1987	3.741010E-06
110	8	20	10	1987	3.431296E-06
118	11	50	38	1987	2.773803E-06
118	12	5	37	1987	2.815076E-06
118	12	13	7	1987	2.938583E-06
118	12	28	7	1987	2.942451E-06
118	12	35	37	1987	2.798537E-06
118	12	50	37	1987	2.939385E-06
124	6	37	39	1987	2.771442E-06
124	6	52	38	1987	2.963679E-06
124	7	0	8	1987	2.998537E-06
124	7	15	8	1987	2.963223E-06
124	7	22	38	1987	2.798582E-06
124	7	37	37	1987	2.822870E-06

Table A.4. (continued)

Day	Hour	Minute	Second	Year	Square of root mean square
131	7	31	12	1987	2.467943E-06
131	7	46	11	1987	2.458109E-06
131	7	53	41	1987	2.440712E-06
131	8	8	41	1987	2.557286E-06
131	8	16	11	1987	2.699001E-06
131	8	31	11	1987	2.623515E-06
161	10	48	29	1987	1.547588E-06
161	11	3	28	1987	1.535721E-06
161	11	10	58	1987	1.566970E-06
161	11	25	58	1987	1.559029E-06
161	11	33	28	1987	1.496985E-06
161	11	48	28	1987	1.465528E-06
166	11	47	53	1987	1.384891E-06
166	12	2	53	1987	1.432448E-06
166	12	10	23	1987	1.368879E-06
166	12	25	23	1987	1.462360E-06
166	12	32	53	1987	1.394535E-06
166	12	47	53	1987	1.452544E-06
203	6	25	16	1987	1.647110E-06
203	6	40	16	1987	1.599190E-06
203	6	47	46	1987	1.634446E-06
203	7	2	46	1987	1.581128E-06
203	7	10	16	1987	1.782671E-06
203	7	25	16	1987	1.632679E-06

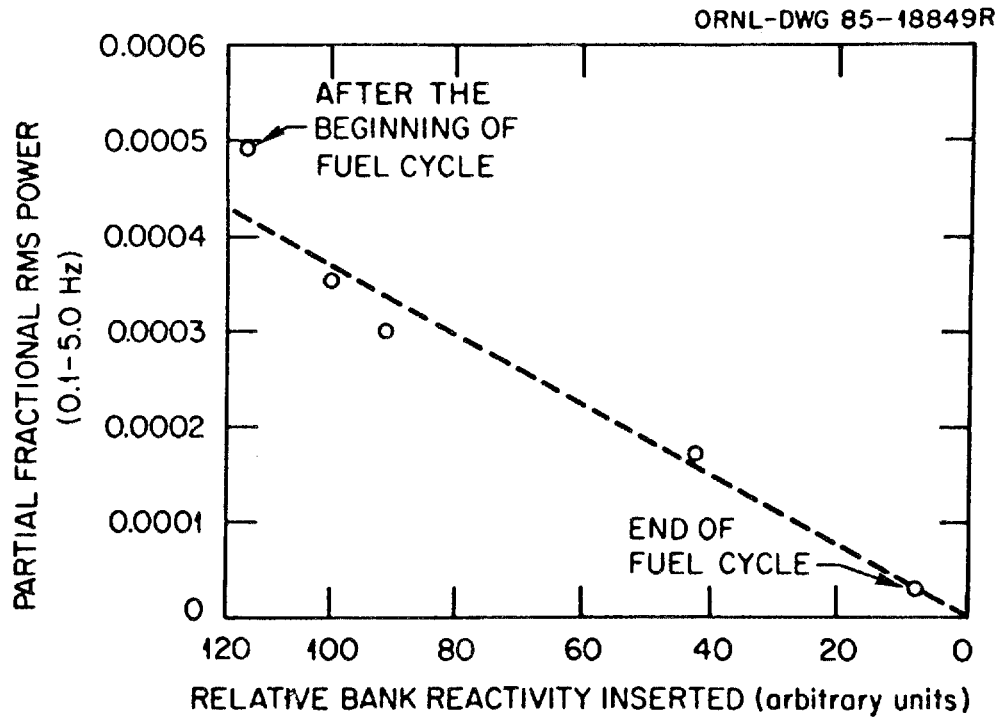


Fig. A.2. The RMS neutron noise due to control rod fluctuation plotted against the relative worth of the inserted bank during the first fuel cycle. A background rms of 0.000195 (found with all rods out) is removed from all data points before plotting.

Table A.5. Example 2 search results^a

Measurement key	CIC-2 % power	Datafile	Measurement key	CIC-2 % power	Datafile
712	90.66	FEB23.DAT	713	91.17	FEB23.DAT
714	91.63	FEB23.DAT	715	91.76	FEB23.DAT
716	91.84	FEB23.DAT	717	92.19	FEB23.DAT
718	92.20	FEB23.DAT	719	92.20	FEB23.DAT
720	92.17	FEB23.DAT	721	92.04	FEB23.DAT
722	92.11	FEB23.DAT	723	92.01	FEB23.DAT
724	91.99	FEB23.DAT	725	91.86	FEB23.DAT
726	91.64	FEB23.DAT	727	91.67	FEB23.DAT
728	91.69	FEB23.DAT	729	91.73	FEB23.DAT
730	91.55	FEB23.DAT	731	91.45	FEB23.DAT
732	91.72	FEB23.DAT	733	92.74	FEB23.DAT
734	93.81	FEB23.DAT	735	95.05	FEB23.DAT
736	95.86	FEB23.DAT	737	96.86	FEB23.DAT
738	97.87	FEB23.DAT	739	98.88	FEB23.DAT
740	99.28	FEB23.DAT	741	100.30	FEB23.DAT
742	100.90	FEB23.DAT	743	100.70	FEB23.DAT
744	100.60	FEB23.DAT	745	100.30	FEB23.DAT
746	100.60	FEB23.DAT	747	100.40	FEB23.DAT
748	100.30	FEB23.DAT	749	100.40	FEB23.DAT
750	100.20	FEB23.DAT	751	100.10	FEB23.DAT
752	100.30	FEB23.DAT	753	99.93	FEB23.DAT
754	100.10	FEB23.DAT	755	96.46	FEB23.DAT
756	96.36	FEB23.DAT	757	92.65	FEB23.DAT
758	92.70	FEB23.DAT	759	86.75	FEB23.DAT
760	85.53	FEB23.DAT	761	80.36	FEB23.DAT
762	79.49	FEB23.DAT	763	74.43	FEB23.DAT
764	74.00	FEB23.DAT	765	73.68	FEB23.DAT
766	68.13	FEB23.DAT	767	67.62	FEB23.DAT
768	67.19	FEB23.DAT	769	60.30	FEB23.DAT
770	60.13	FEB23.DAT	771	59.72	FEB23.DAT
772	59.55	FEB23.DAT	773	59.53	FEB23.DAT
774	59.53	FEB23.DAT	775	59.34	FEB23.DAT
776	59.43	FEB23.DAT	777	59.39	FEB23.DAT
778	59.25	FEB23.DAT	779	59.24	FEB23.DAT
780	59.47	FEB23.DAT	781	59.47	FEB23.DAT

Table A.5. (continued)

Measurement key	CIC-2 % power	Datafile	Measurement key	CIC-2 % power	Datafile
782	59.43	FEB23.DAT	783	59.45	FEB23.DAT
784	59.40	FEB23.DAT	785	59.44	FEB23.DAT
786	59.27	FEB23.DAT	787	59.30	FEB23.DAT
788	59.32	FEB23.DAT	789	59.27	FEB23.DAT
790	59.33	FEB23.DAT	791	59.35	FEB23.DAT
792	59.65	FEB23.DAT	793	62.53	FEB23.DAT
794	62.45	FEB23.DAT	795	62.51	FEB23.DAT

^aCIC = compensated ion chamber.

INTERNAL DISTRIBUTION

- | | |
|---------------------|--------------------------------------|
| 1. S. J. Ball | 14. J. D. Stiegler |
| 2. L. F. Blankner | 15. R. E. Uhrig |
| 3. H. R. Brashear | 16. J. D. White |
| 4. C. R. Brittain | 17. R. T. Wood |
| 5. N. E. Clapp, Jr. | 18. B. Chexal, Advisor |
| 6. B. Damiano | 19. V. Radeka, Advisor |
| 7. B. G. Eads | 20. R. M. Taylor, Advisor |
| 8. D. N. Fry | 21-22. Central Research Library |
| 9. K. Korsah | 23. Y-12 Technical Reference Section |
| 10. D. W. McDonald | 24-25. Laboratory Records |
| 11. D. R. Miller | 26. Laboratory Records-Record Copy |
| 12. J. A. Mullens | 27. ORNL Patent Section |
| 13. R. L. Shepard | 28. I&C Division Publications Office |

EXTERNAL DISTRIBUTION

29. Assistant Manager for Energy Research and Development, DOE-OR,
P.O. Box 2001, Oak Ridge, TN 37831-8600
30. H. Alter, Office of Technology Support Programs, NE-462, U.S. DOE,
Washington, D.C. 20585
31. L. R. Campbell, Westinghouse Hanford, P.O. Box 1970, NZ-32, Richland,
WA 99352
32. J. W. Daughtry, Westinghouse Hanford, P.O. Box 1970, NZ-32, Richland,
WA 99352
33. D. J. Swain, Westinghouse Hanford, P.O. Box 1970, NZ-32, Richland,
WA 99352
34. J. A. Thie, 12334 Bluff Shore Drive, Knoxville, TN 37922
- 35-36. Office of Scientific and Technical Information, P.O. Box 62, Oak Ridge,
Tennessee 37831.

